

1 Reviewer 2
2 I am satisfied with the answers the authors gave me and the additions made to the manuscript. Therefore, I recommend
3 the consideration for publication in Geoscientific Model Development.
4 I only have a few corrections (lines refer to the the tracked-changes version of the manuscript).
5
6 L551 "over orography": shouldn't that be "over complex orography"?
7 *Corrected*
8 L668 data "were".
9 *Corrected*
10 L676 "we repeated" since "we repeat" since past tense is used in the whole paragraph.
11 *Corrected*
12 L838 "repeat the analysis using the MESAN reanalysis as reference" better than "repeat results".
13 *Edited accordingly*
14 L855, L925 "RCM-dependent"
15 *Ok*
16 L877 "therefore those results are not shown" better than "and so are not shown"
17 *Corrected*
18 L110 "at the end of the process" is not necessary, in my view, since you already refer to the u-chronic dataset.
19 *Edited accordingly*
20 L1104, L1106 "aproaches" better than "techniques".
21 *Edited accordingly*
22 L1119 "downscaling effects generally seem to be the most important" better than "it generally seems to be downscaling
23 effects that are the most important".
24 *Edited accordingly*
25 L1129 "smoothing" better than "averaging".
26 *Ok*
27 L1170 which "other studies"?
28 *I have added the example of Prein and Gobiet 2017*
29 L1198 "reanalysis-based".
30 *Ok*
31

32 **The benefits of increasing resolution in global and regional** 33 **climate simulations for European climate extremes**

34 Carley E. Iles¹, Robert Vautard¹, Jane Strachan², Sylvie Joussaume¹, Bernd R. Eggen² and Chris
35 D. Hewitt^{2,3}

36 ¹Laboratoire des Sciences du Climat et de l'Environnement, LSCE/IPSL, CEA-CNRS-UVSQ, Université
37 Paris-Saclay, F-91198 Gif-sur-Yvette, France

38 ²~~Hadley Centre~~, Met Office [Hadley Centre](#), Exeter, UK

39 ³[Centre for Applied Climate Sciences, University of Southern Queensland, Toowoomba, Australia.](#)

40 *Correspondence to:* Carley E. Iles (carley.iles@lsce.ipsl.fr)

41 **Abstract.** Many climate extremes, including heatwaves and heavy precipitation events, are projected to worsen under
42 climate change, with important impacts for society. Future projections, required for adaptation, are often based on
43 climate model simulations. Given finite resources, trade-offs must be made concerning model resolution, ensemble
44 size and level of model complexity. Here we focus on the resolution component. A given resolution can be achieved
45 over a region using either global climate models (GCMs) or at lower cost using regional climate models (RCMs) that
46 dynamically downscale coarser GCMs. Both approaches to increasing resolution may better capture small-scale
47 processes and features (downscaling effect), but increased GCM resolution may also improve the representation of the
48 large-scale atmospheric circulation (upscaling effect). The size of this upscaling effect is therefore important for
49 deciding modelling strategies. Here we evaluate the benefits of increased model resolution for both global and regional
50 climate models for simulating temperature, precipitation and wind extremes over Europe at resolutions that could
51 currently be realistically used for coordinated sets of climate projections at the pan-European scale. First we examine
52 the benefits of regional downscaling by comparing EURO-CORDEX simulations at 12.5 and 50 km resolution to their
53 coarser CMIP5 driving simulations. Secondly, we compare global scale HadGEM3-A simulations at three resolutions
54 (130, 60 and 25 km). Finally, we separate out resolution dependent differences for HadGEM3-A into downscaling and
55 upscaling components using a circulation analogue technique. Results suggest limited benefits of increased resolution
56 for heatwaves, except in reducing hot biases over mountainous regions. Precipitation extremes are sensitive to
57 resolution, particularly over complex orography, with larger totals and heavier tails of the distribution at higher
58 resolution, particularly in the CORDEX vs CMIP5 analysis. CMIP5 models underestimate precipitation extremes,
59 whilst CORDEX simulations overestimate compared to E-OBS, particularly at 12.5 km, but results are sensitive to the
60 observational dataset used, with the MESAN reanalysis giving higher totals and heavier tails than E-OBS. Wind
61 extremes are somewhat stronger and heavier tailed at higher resolution, except at coastal regions where large coastal
62 grid boxes spread strong ocean winds further over land. The circulation analogue analysis suggests that differences
63 with resolution for the HadGEM3-A GCM are primarily due to downscaling effects.

64

65 **1 Introduction**

66 Climate extremes, such as heatwaves and heavy precipitation events are projected to worsen under climate change,
67 with important impacts for society (Seneviratne et al., 2012). Such projections are generally based on numerical climate
68 model simulations. However, given finite computational resources, trade-offs between model resolution, ensemble size
69 and the level of model complexity are necessary. For extreme events driven by large-scale processes such as stationary
70 anticyclones, the proper simulation of the amplitude of extremes is limited by dynamics but also by land-atmosphere
71 feedbacks and the many physical processes involved in the surface energy budget. Such extremes are typically heat
72 waves, droughts and cold spells. Many other types of extreme event are by nature small scale, i.e. on the order of a
73 few kilometres to a few hundred kilometres. Such is the case of convective precipitation, flash floods, extratropical
74 wind storms, cyclones and medicanes. These are poorly resolved at the resolution of Global Climate Models (GCMs)
75 in CMIP5 (Coupled Model Intercomparison Project Phase 5; Taylor et al., 2012). Increased resolution in GCMs may
76 improve the representation of small-scale processes and features, including orography and coastlines (downscaling
77 effect), but potentially may also improve the representation of the interaction between small and large scale dynamical
78 processes and ultimately improve the large-scale atmospheric flow (upscaling effect). For instance, a better
79 representation of baroclinic eddies may help to better simulate large Rossby waves such as those inducing long-lived
80 anomalies, due to the inverse energy cascade. This may improve the simulation of the frequency and duration of heat
81 waves and cold spells, and related anomalies such as summer droughts. For precipitation and wind extremes, an
82 improvement with resolution could be expected due to the small-scale processes and features involved, including
83 convection and the influence of topography. However, upscaling effects may also have benefits by improving storm-
84 track location, and duration of wet spells. An alternative approach to increasing the resolution of global-scale models
85 is to use regional climate models (RCMs) driven by coarser GCMs to achieve a given high resolution over a limited
86 area at lower cost. However, this technique only captures downscaling effects, since the RCM inherits the large scale
87 circulation from the driving GCM.

88
89 Current generation GCMs commonly used for climate projections (e.g. CMIP5 models) have a horizontal grid spacing
90 ranging from about 70 to 250 km. Resolution has been increasing further in CMIP6 (Eyring et al. 2016), with some 25
91 km simulations now being run under projects such as PRIMAVERA and HighResMIP (part of CMIP6; Haarsma et
92 al., 2016). For coordinated RCM experiments, such as CORDEX (Coordinated Regional Downscaling Experiment;
93 Giorgi et al., 2009), grid spacing is generally between 10 to 50 km (e.g. Jacob et al., 2014). In order to simulate
94 convective precipitation a grid spacing of <5 km is needed, which is very computationally expensive, but such
95 ensembles of convection permitting RCMs are currently in development (e.g. Coppola et al., 2019; Risanto et al. 2019).
96 An important question is the extent to which increased resolution benefits the simulation of extreme events for both
97 global and regional models for the kind of resolutions that can realistically be run for coordinated pan-continental
98 climate projections. Particularly, whether using global high resolution adds further benefits over regional high
99 resolution due to an improved large scale circulation. We will address these questions focusing on Europe, for which
100 a large number of coordinated RCM simulations at two standard resolutions are available as part of the EURO-
101 CORDEX initiative (Jacob et al., 2014), and whose climate is highly variable and affected by a range of both large and

102 small scale processes, which present challenges for adequate simulation. We focus on extreme precipitation,
103 temperature and wind, to cover a range of phenomena that may be affected by resolution in different ways. Throughout
104 the rest of this manuscript we use the term “resolution” to mean model horizontal grid spacing, whilst recognising that
105 a model’s effective resolution, in terms of the scales it can capture, is always coarser than its grid spacing (Skamarock
106 2004; Klavar et al. 2020).

107
108 The benefits of increased resolution for European precipitation extremes are well documented, whilst the effects on
109 heatwaves, cold spells and wind extremes are less well known. In GCMs, global precipitation tends to increase with
110 resolution, and for grid point GCMs (as opposed to spectral GCMs) the fraction of land precipitation and moisture
111 fluxes from land to ocean increases, largely due to better resolved orography (Vannière et al., 2019; Terai et al., 2018;
112 Demory et al., 2014). Precipitation extremes tend to get heavier and in some studies agree better with observational
113 estimates with increased resolution (Wehner et al., 2010, O’Brien et al., 2016; Kopparla et al., 2013; Shields et al.,
114 2016; Vannière et al., 2019; Demory et al. 2020; Strandberg and Lind 2020), unless the parameterisation schemes are
115 not suited to the resolution (e.g. Wehner et al., 2014 and possibly Bador et al. 2020, who found worse performance in
116 higher resolution versions of multiple GCMs whose parameterisations were not retuned at higher resolution,
117 particularly in the tropics). In Europe, Schiemann et al. (2018) find that both mean and extreme precipitation are
118 simulated better with increased resolution in HadGEM3A, mostly originating from better resolved orography. In
119 contrast, Van Haren et al. (2015a) find that improvements in Northern and Central European mean and extreme winter
120 precipitation with resolution are mostly associated with improved storm tracks in EC-Earth. For RCMs, extreme
121 precipitation is improved with resolution when compared to high resolution observations, particularly over complex
122 orography, including frequency-intensity distributions and spatial patterns, (e.g. Torma et al., 2015; Prein et al., 2016;
123 Ruti et al., 2016; Fantini et al. 2018). However, benefits are smaller for regional and seasonal mean precipitation.
124 Convection permitting models (<4km grid spacing) are particularly beneficial in simulating summer extreme and sub-
125 daily precipitation, including the diurnal cycle of convection, but can overdo extreme precipitation (e.g. Prein et al.,
126 2015; Kendon et al., 2012; 2014).

127
128 For heatwaves, increasing horizontal resolution does not lead to obvious benefits in RCM simulations (see e.g. Vautard
129 et al., 2013 for EURO-CORDEX), except improved spatial detail (Gutjahr et al., 2016). However, increased resolution
130 may have more impact in global models since the large scale circulation that contributes to heatwave formation may
131 be affected. This remains a largely unstudied question, with the exception of a few studies such as Cattiaux et al. (2013)
132 who find that increasing resolution in the IPSL GCM leads to a reduction in the cold bias of both cold and warm
133 extremes in Europe, along with improved statistics, such as duration and frequencies and improved weather regimes.

134
135 For wind extremes, stronger winds and better spatial detail with resolution have been found for regional models (e.g.
136 Pryor et al., 2012; Kunz et al., 2010). Donat et al. (2010) found that observed storm loss estimates for Germany could
137 be reconstructed more accurately through dynamical downscaling compared to using the coarser resolution driving
138 ERA-40 data directly. Ruti et al., (2016) found improvements in Mediterranean cyclogenesis in coupled Med-
139 CORDEX RCMs relative to the ERA-interim driving data, whilst extreme winds over the Mediterranean generally

140 improve (i.e. are stronger) with higher resolution RCMs (e.g. Ruti et al. 2016; Hermann et al. 2011). Most GCM studies
141 focus on the simulation of extratropical cyclones rather than wind directly. Such studies find an improvement in the
142 representation of various aspects of Northern Hemisphere extratropical cyclones with increased resolution, including
143 frequency, intensity and the position of the storm tracks (Colle et al., 2013; Jung et al., 2006; 2012), even in the higher
144 resolution CMIP5 models ($\sim < 130$ km; Zappa et al., 2013). Vries et al., (2019) found that the resolution of Atlantic
145 Gulf-Stream SST fronts affects winter extratropical cyclone strength. Gao et al (2020) found that explosively
146 intensifying “bomb” extratropical cyclones are more frequent and associated with stronger winds in higher resolution
147 GCMs. Whether the aforementioned improvements translate into an improvement in wind extremes remains to be
148 assessed.

149
150 Persistence of weather regimes, such as blocking or the phase of the North Atlantic Oscillation, can be important
151 drivers for extreme events in Europe. Using the ECMWF IFS model, Dawson et al., (2012; 2015) find that such weather
152 regimes cannot be simulated realistically at typical CMIP5 resolution (~ 125 km grid spacing), but are improved at 40
153 km, and well-simulated at 16 km. Cattiaux et al., (2013) find improvements at more modest resolutions in the IPSL
154 model. However, multi model GCM analyses by Strommen et al. (2019) and Fabiano et al. (2020) suggest that only
155 some aspects of weather regimes are systematically improved with resolution, and that these aspects are not consistent
156 between atmosphere only or coupled GCMs. Blocking frequency tends to be underestimated by CMIP5-resolution
157 climate models (Anstey et al., 2013). This tends to be somewhat improved with resolution, particularly over the North
158 Atlantic (Jung et al., 2012, Anstey et al., 2013; Matsueda et al., 2009, Berckmans et al., 2013, Davini et al., 2017a;
159 2017b; 2020; Strommen et al. 2019; Schiemann et al. 2020), although results tend to be somewhat sensitive to season
160 and model considered (Schiemann et al., 2017) and compensating errors may be involved (Davini et al., 2017a for EC-
161 EARTH). O’Reilly et al. (2016) find that having a well-resolved Gulf stream SST front is also important for European
162 winter blocking and associated cold spells. An important question is whether these improvements in the large scale
163 circulation translate into an improvement in the simulation of European climate extremes.

164
165 Here we examine the benefits of increased resolution for global and regional models for the simulation of European
166 temperature, precipitation and wind extremes. We further break down any resolution related differences for a global
167 model into upscaling and downscaling components. This will shed light on whether potential improvements in the
168 large scale circulation suggested in the literature translate into an improved representation of climate extremes. This is
169 an important consideration in choosing how to distribute finite resources between global and regional models. We
170 focus on the kind of models widely used to provide climate projections at a European scale, applying a consistent
171 approach across model types. Firstly, the benefits of regional dynamical downscaling are explored by comparing
172 EURO-CORDEX simulations at 50 and 12.5 km resolutions to their coarser driving CMIP5 GCMs. Secondly, the
173 benefits of increased resolution for a global model are examined using HadGEM3-A at 130, 60 and 25 km resolution.
174 Finally, the roles of upscaling versus downscaling will be examined using a circulation analogue technique applied to
175 HadGEM3-A.

176 **2 Observational and model data**

177 **2.1 Observational data**

178 Model simulations are evaluated using observational and reanalysis datasets. For daily precipitation and daily
179 maximum temperature, we use the gridded station based dataset E-OBS v15 on a 0.5° latitude-longitude grid (Haylock
180 et al. 2008). This covers the European domain from 1950 to present. Gridded datasets tend to reduce the magnitude of
181 extremes compared to station data through smoothing effects, but are more comparable to the grid box averages from
182 GCMs (Haylock et al. 2008). E-OBS has a somewhat non-uniform underlying station density, with relatively high
183 densities in Germany, Sweden and Slovenia, and low densities in other countries (e.g. Spain, France, Austria). It tends
184 to underestimate precipitation extremes relative to higher density regional datasets, especially where it has poor
185 coverage, due to missed extremes which are local in scale (Prein and Gobiet 2017; Herrera et al. 2019). However, such
186 high resolution datasets are not available at a pan-European scale. As a compromise, results are repeated for
187 precipitation extremes using the 5.5 km resolution MESAN reanalysis (Landelius et al. 2016), which adjusts a
188 downscaled first guess from the 22km resolution HIRLAM reanalysis (Dahlgren et al. 2016) with a network of station-
189 based precipitation observations. For much of Europe these are the same as those used for E-OBS, but with the addition
190 of Swedish Meteorological and Hydrological Institute (SMHI) stations over Sweden, and a high density of Meteo-
191 France stations over France (Landelius et al. 2016). MESAN provides daily precipitation data for the more limited
192 period 1989-2010. Prein and Gobiet (2017) find that it gives heavier extremes than E-OBS in some regions (France,
193 Spain, the Carpathians), but generally not as high as the high resolution regional datasets (except in France). Neither
194 dataset is corrected for gauge undercatch, which tends to be around 3-20% for rain, and up to 40% for snow, or even
195 80% for non-shielded gauges (Førland and Institutt 1996; Goodison et al. 1997).

196
197 Wind extremes tend to happen on sub-daily time scales, necessitating the use of sub-daily data to avoid missing as
198 many events (although events, or their peak magnitude, will still be missed). We use 10 m wind speed from three
199 reanalysis datasets. These are the EURO4M DYNAD (Landelius et al. 2016), UERRA MESCAN-SURFEX (Bazile et
200 al. 2017) and ERA5 (Hersbach et al. 2019) reanalyses. The former is available at 6 hourly intervals on a 5.5km rotated
201 grid over Europe for the period 1979-2013 and is computed through dynamical adaptation of a downscaled version of
202 the 22km resolution HIRLAM reanalysis to 5.5 km resolution orography using DYNAD (a simplified version of
203 HIRLAM). MESCAN is also available at the same spatial and temporal resolution over Europe from 1961 onwards,
204 but is computed through dynamical downscaling of the 11 km UERRA-HARMONIE reanalysis. Both HIRLAM and
205 UERRA-HARMONIE are forced by the ERA interim global reanalysis (ERA40 before 1979 for the latter). Finally,
206 ERA5 is available globally at 0.25° and at hourly resolution from 1979 onwards. We sub-sample ERA5 to 6 hourly
207 data by taking every sixth value in order to be consistent with the other reanalyses.

208

209 2.2 Climate model data

210 2.2.1 EURO-CORDEX and CMIP5

211 In order to examine the effect of dynamical downscaling for climate extremes, we make use of the EURO-CORDEX
212 (Jacob et al. 2014) RCM simulations for the historical period over the European domain which are driven by lower
213 resolution global scale coupled CMIP5 GCMs. The GCMs are forced by observed records of anthropogenic and natural
214 forcings, such as greenhouse gases, anthropogenic aerosols, land use changes, solar variability and volcanic aerosols
215 to allow comparability to historical records. For the most part the RCMs inherit the effects of these forcing agents from
216 the GCMs, with the exception of greenhouse gases, which are prescribed. A comparison of the RCM simulations with
217 their driving CMIP5 simulations allows us to identify any value added by regional high resolution. The EURO-
218 CORDEX simulations are available at 0.11° and 0.44° (12.5 km and 50 km respectively), allowing an assessment of
219 the difference that increased regional resolution brings. Simulations are performed with the same model versions and
220 parameterisations for both resolutions, except for REMO where rain advection is used at 0.11° but not 0.44° (Kotlarski
221 et al. 2014). By examining the subset of GCM-RCM combinations that are common to both CORDEX resolutions
222 along with their driving GCMs we can isolate the effects of changing resolution. Hereafter, this subset is referred to as
223 the “common subset”. We also examine how representative the results for this common subset are by recalculating
224 them using all available CMIP5 and CORDEX simulations, using one member per model.

225
226 Daily precipitation (pr), daily maximum temperature (tasmax), and 3 hourly wind (sfcWind) were taken from both
227 CORDEX and CMIP5. For wind, every other time step was taken in order to obtain 6 hourly data to be consistent with
228 the reanalysis data. The simulations used are shown in Table S1. These consist of 23 and 19 simulations for
229 precipitation for the 0.44° and 0.11° CORDEX simulations respectively, with 15 in the common subset; 22 and 18
230 respectively for temperature, with 14 in the common subset. For wind, data were very limited for CORDEX at 0.44°
231 and there was no overlap of models with those used for the 0.11° simulations. Therefore, the wind analysis in the main
232 manuscript is based only on CORDEX 0.11° and CMIP5. There were 31 simulations for wind for CORDEX 0.11°,
233 with 15 in the common subset. CORDEX 0.11° and 0.44° were compared instead using the variable sfcWindmax (daily
234 maximum wind) which was available for 9 models at both resolutions (see Figure S8). There seemed to be
235 inconsistencies in the way sfcWindmax was calculated between CMIP5 models (mostly yielding stronger annual
236 maximum winds compared to using 3 hourly data to varying extents, but sometimes weaker), which precluded basing
237 the full analysis on this variable. When calculating ensemble medians for the common subset of simulations, we
238 repeated GCM members that drive more than one RCM. The number of CMIP5 simulations used for the extended
239 ensemble was 44 for precipitation, 42 for temperature and 25 for wind.

240

241 2.2.2 UPSCALE simulations

242 In order to examine the benefits or otherwise of differences in resolution for a global model, we make use of simulations
243 undertaken as part of the UPSCALE project (UK on PRACE: weather-resolving Simulations of Climate for globAL
244 Environmental risk; Mizielinski et al. 2014). This consists of the atmosphere only version of the Hadley Centre Global

245 Environment Model 3 (HadGEM3-A) run at three different resolutions: N96 (130 km), N216 (60 km) and N512 (25
246 km), all with 85 vertical levels for the period 1985-2011, with 5, 3 and 5 ensemble members respectively (or 3, 3 and
247 5 for wind data). The simulations are forced by observed records of greenhouse gases, aerosols, ozone, solar variability
248 and volcanic forcings following the AMIP-II procedure (Taylor et al. 2000), but using the higher resolution OSTIA
249 analysis (Operational Sea Surface Temperature and Sea Ice Analysis) for sea surface temperatures (SSTs) and sea ice
250 (Donlon et al. 2012). Very few parameters differ between the resolutions, enhancing the comparability of the three
251 ensembles. We use daily precipitation data, daily maximum temperatures and 3-hourly wind (subsampled to 6-hourly).

252 **2.3 Regridding**

253 In order to compare models of different resolutions with each other and with the observational datasets it was necessary
254 to regrid variables to a common grid. Using a high resolution grid for evaluation would preserve the finer spatial detail
255 and localised extremes for high resolution simulations, but is sometimes considered unfair for coarse resolution models
256 which cannot be expected to simulate the same intensities of extremes even for a perfect simulation due to spatial
257 smoothing effects. If processes are captured better at higher resolution, improvements should still be visible when
258 regridded to coarser resolution (Prien et al. 2016; Fantini et al. 2018). However, the finer spatial detail is an inherent
259 advantage of high resolution and smoothing this out will result in partial information loss. We use the 0.5° regular
260 longitude-latitude grid of E-OBS since it is in-between the resolution of the CORDEX models and CMIP5, and is
261 computationally feasible. Some of the benefits of higher resolution may be lost by doing this, putting our results on
262 the conservative side. Nevertheless, sensitivity tests showed that results for MESAN did not change perceptibly by
263 using a 0.5° grid compared to a 0.1° grid. We regrid the daily data, before the calculation of annual extreme indices.

264
265 The sensitivity of the results to the regridding technique was investigated for a number of models of different
266 resolutions and compared to results based on using the original grids (Figure S1). For the coarser resolution models
267 (e.g. HadCM3) results for precipitation extremes were particularly sensitive to the regridding technique, with much
268 weaker extremes for some techniques e.g. distance-weighted average remapping and bilinear interpolation, with
269 unrealistic artefacts in the spatial patterns for many methods. For high resolution models, the regridding technique did
270 not make much difference to the results, although conservative remapping tended to dampen extreme precipitation,
271 particularly for CORDEX 0.11. Overall the nearest neighbour method was chosen for precipitation for everything
272 except CORDEX 0.11 and MESAN since it gave results very close to using the original grid for all model resolutions,
273 preserving the amplitude of extremes, and also having minimal artefacts when plotting spatial patterns of precipitation
274 extremes. For going from high to lower resolution (e.g. 0.11° to 0.5°) nearest neighbour is less appropriate since
275 information from only a subset of grid cells is incorporated. Therefore, bicubic remapping was used for CORDEX 0.11
276 and MESAN, which also replicated results using the original grid very well (Figure S1). Wind and temperature results
277 were also somewhat sensitive to regridding technique, particularly for the coarser models. The above choices also
278 seemed appropriate for these variables (nearest neighbour in most cases, but bicubic for CORDEX 0.11, MESCAN,
279 ERA5 and DYNAD), both in terms of replicating return period results using the original grid, and retaining the blocky
280 nature of the low resolution simulations in the spatial patterns.

281 **3 Methods**

282 **3.1 Extremes Indices**

283 In order to examine extremes, we adopt indices based on the ETCCDI indices (Zhang et al. 2011). For precipitation
284 these are the annual maximum daily precipitation (Rx1day) and the annual maximum consecutive 5-day total
285 (Rx5day). For temperature we use the annual maximum daily maximum temperature (TXx) and the annual maximum
286 consecutive 5-day mean of daily maximum temperature (TXx5day). Rx1day and TXx5day are presented in the figures,
287 whilst the other indices are commented on in the text. For wind we use the annual maximum of daily maximum wind,
288 which we refer to as (WindXx). This is based on 6-hourly data. These are therefore much rarer extremes than those
289 based e.g. on the 95th or even 99th percentile which would happen on average 1 in 20 days and 1 in 100 days
290 respectively. One drawback is that this makes robust statistics more challenging.

291
292 In order to examine how well the climate models simulate extremes and the differences between different resolutions,
293 we first examine the spatial patterns of the climatological mean values of the indices and their biases with respect to
294 observational datasets. We then examine return period plots (see definitions below) for a number of regions for each
295 index, which highlights any differences in the shape of the tails of the distribution of the extremes. The regions used
296 are based on the PRUDENCE regions (Christenson and Christenson 2007) and the IPCC SREX regions (Seneviratne
297 et al. 2012) and are shown in Figure S2 and Table S2. A subset of representative regions are presented here, with some
298 comments about the others.

299 **3.2 Return periods**

300 In order to calculate regional return periods and return values we first sort the data into ascending order for each grid
301 cell. The return periods are calculated as N/k where N is the number of years of data, and k is the rank, with $k=1$ for
302 the largest value. Return periods are therefore the inverse of the probability of an event exceeding a given value (called
303 the “return value”). This is an empirical approach and has the limitation that return periods cannot exceed the number
304 of years of data used (e.g. 36 years). This is still the case even if an extremely unusual event occurs. Fitting a GEV
305 would allow estimates for higher return periods, but this would still be an extrapolation. The area weighted regional
306 average is made, for given return periods, over the associated return values. To avoid complications from missing data,
307 grid cells in E-OBS with more than 5 days of missing data in any year during the period examined were masked for
308 the whole period. Having one or more years missing would complicate the calculation of regional mean return periods
309 and values. Models and observational datasets are masked to have the same spatial coverage, which is land only. A
310 common time period across the models being examined and the observations they are being compared to is chosen to
311 allow comparability. For the CMIP5 and CORDEX analysis 1970-2005 is used for temperature and precipitation and
312 1979-2005 for wind. For the UPSCALE runs we use 1985-2011 for temperature, and 1989-2010 for precipitation to
313 allow comparisons with MESAN (1986-2011 is used for the analogue analysis, see below) and 1986-2011 for wind.

314
315 In order to allow the shapes of the return period curves to be compared more easily between different types of models
316 (i.e. CMIP5 and CORDEX at both resolutions), we first adjust each model to have the same climatological mean value

317 of the extreme index in question. This effectively shifts the curves up or down, but does not change their shape, which
318 is the focus of these figures. Without such a shift, curves are too spread out to be able to discern differences in shape.
319 Therefore we cannot comment on mean biases of the extremes indices based on the return plots, but these biases are
320 already shown and discussed based on map figures (see section 3.1). We implement this adjustment by subtracting the
321 difference between the model climatology of the index in question and the climatology of the reference observational
322 dataset for each model at a grid cell level. We use E-OBS as the reference for temperature and precipitation, and
323 MESCAN for wind. The additional observational datasets shown in the return period plots are also adjusted in the
324 same way. For the UPSCALE simulations, results can also be examined without the need to shift the curves to a
325 common mean value because the same version of the same model is used for a given resolution, meaning that curves
326 for individual simulations tend to cluster together instead of having large mean differences. In this way, differences in
327 biases with resolution are also seen in the return period plots. Nevertheless, we also present UPSCALE results with
328 the adjustment in Figure S10 for comparison.

329
330 Confidence intervals for the observational datasets are calculated using a bootstrapping method. If, for example, the
331 analysis period was 1970-2005 (i.e. 36 years), 1000 random samples of 36 years from this period are chosen from the
332 same dataset, allowing the same year to be chosen more than once per iteration. For each random sample, the chosen
333 values are sorted for each grid cell and a regional average is calculated as above, effectively yielding 1000 return period
334 curves per region. The 5th and 95th percentile of these values are then calculated to give the confidence intervals.

335

336 **4 Results**

337 **4.1 The benefits of regional high resolution: EURO-CORDEX versus CMIP5**

338 **4.1.1 Temperature extremes**

339 Figure 1 shows the spatial patterns of the climatological mean of TXx5day for the period 1970-2005 for E-OBS, and
340 the multi-model medians (MMM) of CMIP5, and CORDEX at both resolutions, along with their biases with respect
341 to E-OBS. The same general pattern can be seen in both E-OBS and the models, with hotter extremes in the south and
342 cooler extremes in the north and over the mountains. At higher resolution the colder warm extremes over the Alps and
343 Carpathians become more distinct. For the “common subset” the pattern of biases relative to E-OBS is similar for both
344 CMIP5 and CORDEX with cold biases in the North and West and hot biases in the South-East. However, the hot biases
345 over the mountains reduce with higher resolution since the model topography is higher. The cold bias over Scandinavia
346 is also larger in CORDEX than in CMIP5. Biases for CORDEX using the whole ensemble are similar to those for the
347 common subset. For CMIP5 the hot biases over the south-east, and over mountain ranges are stronger when using all
348 simulations compared to the subset. Findings for TXx are similar, but hotter (not shown).

349

350 To give an idea of the level of consistency of results between models, results for individual models are shown in Figure
351 S3. Although the CMIP5 models agree on the general spatial pattern of temperature extremes, their absolute

352 magnitudes vary considerably, although all are too hot over the Alps. There are also substantial differences between
353 results from different RCMs, including those driven by the same GCM, although the driving GCM does seem to affect
354 the overall magnitude of the temperature extremes. Biases of individual RCMs do not appear systematically smaller
355 than that of their driving GCM. Patterns are very similar for the same GCM-RCM chains at the both 12.5 and 50 km
356 resolutions. Results for different ensemble members of the same GCM or GCM-RCM chain are very consistent,
357 suggesting that the differences between models are not due to internal variability.

358
359 In order to assess any effect of resolution on the shape of the tails of the statistical distribution of temperature extremes,
360 Figure 2 (left column) shows return period against magnitude for TXx5day for CMIP5, CORDEX at both resolutions
361 and E-OBS (see Methods). Results are shown for Northern, Central and Southern Europe, and are representative of
362 results for the smaller PRUDENCE regions that fall within their boundaries. There is no obvious difference in the
363 shape of the tails between CMIP5 and CORDEX. Agreement with E-OBS is good for the multi model median, although
364 many individual ensemble members lie outside the range of the observational uncertainty.

365
366 In summary, shapes of return period curves for temperature extremes appear to be insensitive to dynamical
367 downscaling based on comparing CMIP5 to CORDEX at 0.11° and 0.44°, but biases are affected, for instance over
368 mountains where hot biases decrease with resolution.

369 4.1.2 Precipitation extremes

370 Now we consider precipitation extremes for CMIP5 compared to CORDEX. Figure 3 shows the climatological mean
371 of Rx1day for E-OBS and the MMMs of CMIP5 and CORDEX at both resolutions, and their differences with respect
372 to E-OBS. The heaviest annual maximum precipitation totals in E-OBS occur over the Alps and the western side of
373 coastal mountain ranges, including western Norway and north-eastern Spain. A similar spatial pattern of precipitation
374 distribution can be seen in the models, although totals are lower in CMIP5, and higher in CORDEX. CMIP5 is drier
375 than E-OBS over most of Europe, particularly over the areas of maximum observed precipitation (i.e. over or near
376 mountains), whilst CORDEX is generally wetter than observed, particularly in these same locations, and at higher
377 resolution. Results using the entire ensembles are very similar to using the common subset of simulations. Previous
378 studies suggest that E-OBS underestimates precipitation extremes since it is not corrected for gauge undercatch and
379 has a relatively low underlying station density (e.g. Prein and Gobiet 2017). Therefore, we also repeat [the analysis](#)
380 [using the MESAN reanalysis as the reference—results relative to the MESAN reanalysis](#) (Figure S4) for the shorter
381 period 1989-2005. MESAN uses a particularly high density of stations in France (see Data section). The climatology
382 of Rx1day is wetter in MESAN than in E-OBS over most of Europe, most noticeably over the Alps and surrounding
383 areas. This leads to the dry bias in CMIP5 appearing bigger, and the wet bias in CORDEX decreasing, although it is
384 still present in the 0.11° simulations. Using regional-scale very high resolution datasets could improve agreement with
385 the 0.11° simulations, since they tend to give heavier precipitation extremes (Prein and Gobiet 2017). Gauge
386 undercatch will also contribute to the difference, particularly for precipitation extremes associated with strong winds
387 and in snow dominated regions

388
389 Figure S5 shows results for individual models. Again, whilst models agree on the general pattern of precipitation
390 extremes – i.e. wettest over mountains, there are considerable inter-model differences concerning the magnitude,
391 particularly over complex orography. A number of CMIP5 models have too light extremes everywhere, but all
392 underestimate precipitation extremes over mountainous regions to a greater or lesser extent. RCMs systematically
393 simulate heavier precipitation extremes compared to their driving GCMs, particularly over mountains, and these
394 extremes tend to become heavier when moving from 0.44° to 0.11° in most cases. Many of the RCMs have heavier
395 precipitation extremes than seen in E-OBS over much of Europe at 0.44°, although this difference may disappear if
396 compared to MESAN. This difference gets bigger at higher resolution and is largest over mountainous regions. The
397 spatial patterns seem to be very RCM-dependent, with limited influence of biases in the driving GCM. Again results
398 are very consistent between ensemble members of the same models.

399
400 Figure 2 (middle column) shows return period curves for Rx1day for Northern, Central and Southern Europe. There is
401 a clear separation in the tails of the distribution according to resolution, with CMIP5 having the lightest tails, CORDEX
402 0.44 in the middle, and CORDEX 0.11 with the heaviest tails across all regions (including the smaller PRUDENCE
403 regions – not shown). Results using the common subset of models or the full ensembles are similar to each other. E-
404 OBS tends to lie between CMIP5 and CORDEX 0.44 for southern Europe, and closer to CORDEX 0.44 in central and
405 northern Europe. Using MESAN gives slightly heavier tails in all three regions, particularly in southern Europe (Figure
406 S6) and France where station density is highest (not shown), causing the best agreement to occur with CORDEX 0.44
407 everywhere. Results for Rx5day are similar, but with marginally less separation between the resolutions, whilst over
408 Northern and Central Europe the best agreement with E-OBS happens at a slightly higher resolution than for Rx1day
409 – i.e. either with CORDEX 0.44 or the lower end of the range of CORDEX 0.11 (not shown).

410
411 In summary, precipitation extremes are wetter and heavier tailed with higher resolution, especially over mountainous
412 regions. CMIP5 has a dry bias, particularly over mountains, whilst CORDEX tends to be too wet relative to E-OBS,
413 particularly at 0.11°, but results are sensitive to observational dataset used, with wet biases for CORDEX reducing
414 when compared to the higher resolution MESAN dataset.

415 4.1.3 Wind Extremes

416 Finally, we examine annual maximum wind (WindXx). Figure 4 shows the multi model medians of climatological
417 mean annual maximum wind for CMIP5 and CORDEX at 0.11° compared to three reanalysis datasets. Data for
418 CORDEX 0.44° were very limited and did not overlap with the models used at 0.11° - ~~therefore those results and so~~
419 are not shown. The MESCAN and DYNAD reanalyses show strong extreme winds over the UK, the Norwegian
420 mountains and the NW coastline of France through to Denmark. Relatively strong winds are also seen over the Spanish
421 plateau, and a belt of strong winds running zonally across central Europe between somewhat slower winds to the North
422 and South. The datasets differ in the magnitude of the winds, with DYNAD having more contrast between areas of
423 low and high wind. MESCAN should be the more accurate of the two (Tomas Landelius, personal communication).

424 ERA5 has notably slower winds, particularly over mountainous regions, but a similar overall zonal tripole pattern can
425 be seen. Niermann et al (2017) found that MESCAN underestimates extreme winds compared to station data over
426 Germany. ERA5 must therefore underestimate even more. Concerning mean winds, Jourdi er (2020) find that ERA5
427 underestimates wind speed compared to French stations, particularly over mountains.

428
429 The CMIP5 driving model median shows a similar overall pattern of WindXx as the reanalyses, particularly ERA5,
430 with a pattern of weaker winds in the north and south, and a belt of stronger winds in the middle. However, CMIP5
431 does not tend to have stronger winds over mountains like in DYNAD and MESCAN. Using the whole CMIP5 ensemble
432 gives similar results. The CORDEX multi model medians show generally higher wind speeds than CMIP5, and
433 captures the high wind speeds along western coastlines and over some mountainous terrain. Results for the common
434 subset of simulations are similar to those obtained from the complete CORDEX ensembles, except that the latter shows
435 slow wind speeds over the Alps instead of high. This latter feature is very RCM-dependent, and indeed the overall
436 pattern and magnitude of the extreme winds almost entirely reflects the choice of RCM with very little influence of
437 GCM (Figure S7). For some RCMs the zonal tripole pattern is the clearest feature (ALADIN, COSMOcrCLIM), whilst
438 for others it is the high winds over mountains and coastlines (RCA, HIRHAM5). The driving GCMs differ considerably
439 in terms of the magnitude of extreme winds, but have a similar overall pattern to each other (Figure S7). Ensemble
440 members of the same model give very similar results for both CORDEX and CMIP5. Multi-model median biases are
441 dependent on the reanalysis used for reference, with CORDEX 0.11 being close to DYNAD, and CMIP5 being closest
442 to ERA5. In order to compare the two resolutions of CORDEX, results based on sfcWindmax instead of 3 hourly wind
443 are presented in Figure S8 (see methods). Winds are either similar between the two resolutions (e.g. RCA and WRF),
444 or stronger at higher resolution (RACMO, HIRHAM5). Again the overall pattern is very RCM-dependent.

445
446 Figure 2 (right column) shows return period plots for WindXx for CMIP5 and CORDEX at 0.11 . The British Isles
447 are shown instead of Northern Europe, since they are particularly affected by wind extremes, and for comparison with
448 the results for the UPSCALE simulations, where this region shows distinctive results. The distribution of annual
449 maximum sfcWindmax has somewhat heavier tails in CORDEX 0.11 compared to CMIP5, regardless of the subset of
450 models used in calculating the multi-model median in all regions examined. CORDEX 0.11 tends to be closest to
451 DYNAD and MESCAN, whilst CMIP5 is closest to ERA5. Figure S9 shows that when using sfcWindmax, CORDEX
452 0.11 has heavier tails than CORDEX 0.44.

453
454 In summary, winds tend to be somewhat stronger, with somewhat heavier tails at higher resolution, with a large spread
455 between models. Reanalysis datasets give fairly diverse results.

456
457 **4.2 Global high resolution: UPSCALE**

458 We now examine the benefits or otherwise of global high vs. standard resolution simulations for simulating climate
459 extremes. Global high resolution may allow an improved representation of the large scale circulation that cannot be

460 captured by regional models, which may in turn affect the representation of climate extremes. For this we examine the
461 UPSCALE simulations (Mizielinski et al. 2014), which consist of a small ensemble of HadGEM3-A simulations at
462 three different resolutions: 130km (N96), 60km (N216), and 25km (N512) (see Data section).

463 **4.2.1 Temperature extremes**

464 Figure 5 shows the ensemble mean climatological mean of TXx5day for the UPSCALE simulations over the period
465 1985-2011 at all three resolutions, and their biases relative to E-OBS. The same general pattern of hotter extremes in
466 the south and colder in the north and over mountainous regions can be seen at all three resolutions, but temperature
467 extremes are hotter at higher resolution in the south and east, and colder over mountains. The same pattern of biases is
468 seen as for CORDEX and CMIP5 with cold biases in the north and hot in the south-east and over mountains. The
469 mountain biases reduce with higher resolution, as the orography becomes better defined, whilst the hot bias in the SE
470 and SW increases and the northern cold bias improves slightly. A coastal cold bias at low resolution disappears at
471 higher resolution as the model land mask becomes more detailed. Note that the SSTs are prescribed and are the same
472 for all simulations. Results for TXx are similar but hotter (not shown).

473
474 Figure 6 (left column) shows regional return period plots for TXx5day for the UPSCALE simulations. Results are a
475 little less consistent across regions for UPSCALE compared to the CMIP5 vs CORDEX analysis, so we split Northern
476 Europe into the British Isles and Scandinavia, and add the Alps, to better capture regional variations. Since the
477 ensemble means are only based on one model, results are presented without adjusting according to the climatology of
478 TXx5day, although such adjusted results can be seen in Figure S10 and allow differences in the shapes of the tails to
479 be seen more clearly. TXx5day seems to be somewhat hotter with higher resolution over many regions, although this
480 is not always clear cut. The Alps are a notable exception, where the higher elevations with higher resolution give rise
481 to colder temperature extremes. There are notable biases relative to E-OBS, with the models being too cold in the
482 north, especially at low resolution, whilst in the south the colder subset of models (N96, the lowest UPSCALE
483 resolution) agree best with the E-OBS. Over the Alps, again the low resolution simulations agree best with E-OBS,
484 with the warmest temperatures, but this will depend on the height of the meteorological stations. This apparent
485 contradiction to the reduced orographic hot bias with resolution in Figure 5 comes from the stronger cold bias of the
486 surrounding areas at low resolution. Figure S10 shows that differences between the shape of the tails with resolution
487 are not systematic across regions and are mostly small, whilst agreement with E-OBS is good everywhere. Results for
488 TXx are similar.

489
490 In summary, hot biases of temperature extremes over mountains reduce with increased resolution for HadGEM3-A.
491 Elsewhere extremes tend towards getting hotter with resolution, whilst the shapes of the return period curves are
492 insensitive.

493 4.2.2 Precipitation extremes

494 For precipitation, Figure 7 shows the ensemble mean climatological mean of Rx1day for the period 1989-2010 for the
495 three UPSCALE ensembles and their differences relative to E-OBS and MESAN. The overall pattern of Rx1day in the
496 simulations is similar to that in the observational datasets, with heavier precipitation extremes and finer spatial detail
497 with increasing resolution over complex orography. All resolutions have bands of heavy precipitation either side of
498 the Alps, but these move closer together as the Alps become better defined. All simulations are generally wetter than
499 E-OBS across most of Europe. The dry bias over orography in the Alps, Southern Norway and Scottish Highlands
500 reduces with resolution, whilst a wet bias on the southern edge of the Alps and the coastal side of the Dinaric Alps in
501 the Balkans appears instead. Comparing to MESAN instead of E-OBS, the general wet bias disappears, and the dry
502 mountain bias over orography at low resolution increases. The differences between resolutions appear smaller than for
503 the CMIP5 versus CORDEX analysis: all the UPSCALE simulations look most similar to CORDEX at 0.44°.
504 However, UPSCALE does not reach as fine a resolution as CORDEX at 0.11° (25 km vs 12.5 km), and CMIP5 is on
505 average slightly coarser than the N96 simulations. In addition, it should be noted that models with the same nominal
506 resolution do not necessarily have the same effective resolution, and that the effective resolution is always less than
507 the nominal resolution (Skamarock 2004; Klavar et al. 2020). Results are similar for Rx5day (not shown).

508
509 Figure 6 (middle column) shows the return period plots for Rx1day for the three resolutions of UPSCALE ensembles.
510 Slightly heavier precipitation extremes are found at higher resolution in all the regions shown (exceptions are France
511 and Mid Europe- not shown). Although the differences are small, they are more obvious in southern Europe and
512 especially in the Alps. Figure S10 shows that there is not much difference in the shape of the tails for most regions,
513 although there are very slightly heavier tails at higher resolution for southern Europe (more so in the Mediterranean
514 sub region- not shown) and more obvious differences over the Alps in the same direction, both of which are regions
515 where convective precipitation is important. E-OBS tends to lie just below the model simulations for most regions
516 (Figure 6), although it agrees with the models for the British Isles, and is between the low and medium resolution
517 simulations over the Alps. MESAN gives higher values for observed Rx1day which improves agreement in regions
518 where E-OBS lay below the models, and causes a higher resolution subset to agree better in the other regions (Figure
519 6). For the curves that are adjusted to have the same climatological mean, E-OBS tends to lie just on the lower end of
520 the ensemble for most regions, whilst MESAN gives slightly heavier tails and tends to improve agreement with models
521 (Figure S10). Results for Rx5day are broadly similar (except that both observational datasets lie above all the models
522 for the British Isles).

523
524 In summary, precipitation extremes are somewhat wetter and heavier tailed with increasing resolution mostly in
525 southern Europe and the Alps for HadGEM3-A. Dry orographic biases decrease with resolution, but wet biases appear
526 in the south next to mountain ranges instead.

527 **4.2.3 Wind extremes**

528 For wind extremes, Figure 8 shows the spatial patterns of climatological mean annual maximum wind for UPSCALE
529 and the same for three reanalyses. The spatial patterns are similar for the three different model resolutions, with the
530 highest winds over the British Isles and coastal regions, lower wind speeds over the Alps, and the zonal tripole pattern
531 described above. The main differences are that the lower resolution model (N96) has stronger winds around the British
532 Isles and western coastlines. This is likely because the larger coastal grid boxes overlap more with the ocean, which
533 tends to have higher wind speeds, or due to differences in the model land mask itself with resolution. The wind speeds
534 at higher resolution are a little stronger overall, most obviously in the central European zonal belt, and over the Alps
535 and Norwegian mountains. All resolutions show stronger winds than ERA5 over most of Europe. Compared to
536 MESCAN winds are too weak in the northern and southern Europe, particularly over mountainous regions, and a little
537 too strong in between. Relative to DYNAD the pattern of differences is similar as for MESCAN, but with stronger
538 negative differences over the Norwegian mountains and positive differences in other parts of Northern Europe. There
539 are positive coastal biases relative to all reanalyses for the N96 simulations that reduce with increased resolution.

540
541
542 Figure 6 (right column) shows the return period plots for some example regions for annual maximum wind for the
543 UPSCALE simulations, without shifting the climatology. Over all regions examined (except the Mediterranean- not
544 shown), the N512 simulations have stronger winds than the N216 simulations. The position of the curve for N96 is
545 strongly related to how much coastline there is relative to land area per region, e.g. with faster winds than the other
546 simulations over the British Isles and southern Europe, but relatively slower winds over central Europe, and particularly
547 over the Alps. There are fairly large differences between reanalysis estimates, with ERA5 always having the slowest
548 winds, and the model simulations tending to lie between ERA5 and the other two reanalyses for most regions. For the
549 adjusted versions of the return period plots (Figure S10), differences in the shapes of the tails with resolution are
550 generally small, although with marginally heavier tails with increasing resolution over a number of regions, e.g the
551 Alps (not all are shown). MESCAN and DYNAD have slightly heavier tails than ERA5, particularly over the Alps and
552 Southern Europe. The shape of the model curves agree well with all reanalyses over the British Isles, Scandinavia and
553 Central Europe, and lie between ERA5 and the other two reanalyses for the Alps and Southern Europe.

554
555 In summary winds are slightly stronger and heavier tailed at higher resolution in HadGEM3-A, except over coastal
556 areas where large coastal grid boxes at low resolution bring strong ocean winds further over land.

557 **4.3 Upscaling versus downscaling**

558 For the global model results, any differences in the representation of extremes according to resolution could come from
559 either upscaling or downscaling effects. Upscaling effects could include a better representation of the large scale
560 circulation, whilst downscaling allows a better representation of small scale processes, such as convection, and an
561 improved representation of orography and coastlines. In order to investigate which of these effects leads to the
562 differences between the low (N96) and high resolution (N512) HadGEM3-A simulations, we employ a circulation

563 analogue technique (e.g. Vautard et al., 2016), which is frequently used in attribution studies (see e.g. Stott et al., 2016;
564 Cattiaux et al., 2010). The idea is to determine whether the simulation of climate extremes changes between the two
565 resolutions if both were to have the same large scale circulation –i.e. isolating the downscaling effect, or conversely
566 whether circulation differences explain any differences in extreme events whilst circulation-variable (e.g. precipitation)
567 relationships stay the same –i.e. the upscaling effect.

568
569 For each day in the lower resolution simulations we pick the nearest circulation analogue from anywhere in the higher
570 resolution simulations, providing it happens at the right time of year (i.e. within a 30-day window centred on the day
571 of the year in question). We then record the associated temperature, precipitation and wind values from the higher
572 resolution simulations to make a “u-chronic” dataset (e.g. Jézéquel, et al. 2018) that contains data from the high
573 resolution simulations but follows the daily sequence of circulation patterns from the low resolution models. We then
574 repeat the analysis of return periods and value as above. We also do the reverse (find analogues for the N512 circulation
575 in the N96 ensemble and record the N96 temperature). Since results using analogues are not directly comparable to the
576 original results due to the lack of an exact analogue match, we also perform “self-analogues” -i.e. finding circulation
577 analogues for the N96 simulations within the N96 ensemble, (excluding the same year from the same ensemble
578 member) and creating a u-chronic time series, and the same for the N512 ensemble). Comparing the resulting return
579 period curves tells us about the contribution of large-scale circulation and downscaling to differences in extremes
580 between the two resolutions. For example, comparing the N96 self-analogue return curve to the version based on N512
581 circulation but with N96 precipitation shows us the contribution of any differences in the large scale circulation
582 between the resolutions i.e. the upscaling effect. Comparing the N96 self-analogue to the version based on N96
583 circulation with N512 precipitation shows us the downscaling effect – i.e. any difference between the relationship
584 between the large scale circulation and precipitation.

585
586 Analogues are defined using geopotential height at 500 hPa, since this avoids complications relating to surface heat
587 lows associated with heat waves in anticyclonic conditions that occur in summer, whilst also avoiding incomplete data
588 due to mountain ranges. Geopotential height is regridded to a 2° grid using bilinear interpolation. This choice ensures
589 that we are comparing analogues with the same resolution and do not penalise small-scale differences. Similarity
590 between circulation states is quantified using pattern correlation, which is not affected by trends in geopotential height
591 with global warming. For precipitation and wind the European domain used is -16 to 44° E and 34 to 72° N (roughly
592 the same as the domain plotted in the map-based figures). For temperature, a larger domain is used, since the history
593 and trajectory of air masses are important for temperature extremes. This domain is loosely based on the domain used
594 by Cattiaux et al. (2010) and extends over the N. Atlantic as well as Europe, (-62 to 44°E and 24 to 80° N). However,
595 results are very similar if the smaller domain is used (not shown). For the 5-day variables (Rx5day and Txx5day) the
596 u-chronic dataset was smoothed using a 5-day running mean ~~at the end of the process~~. We also tried smoothing the
597 daily geopotential height, precipitation and temperature datasets first and then performing the analogue analysis. The
598 relationship between the different curves was largely consistent between the two ~~approachest~~techniques, but absolute
599 values differed and the shape of the curves changed a little. Results presented here are based on the first
600 ~~technique~~approach.

601
602 Figure 9 shows the results of the analogue analysis. The blue curves show the results for the N512 self-analogues, grey
603 represents the N96 self-analogues, red represents results using the circulation patterns from the N96 runs but with the
604 N512 circulation-variable relationships, and green indicates N512 circulation with N96 circulation-variable
605 relationships. The difference between the blue and red curves (or the grey and green curves) shows the contribution
606 from differences in the large scale circulation with resolution, whilst the difference between the blue and green curves
607 (or the red and grey curves) indicates the downscaling effect.

608
609 For TXx5day downscaling effects are dominant over regions that have a clear difference between resolutions, although
610 circulation differences also have a small effect in some regions such as the British Isles (Figure 9). For Rx1day the
611 different curves are very close together for some regions, making it difficult to discern the relative contributions from
612 upscaling and downscaling. However, for regions with an obvious difference between resolutions, such as the Alps
613 and Southern Europe, ~~it seems to be~~ downscaling effects seem to be the~~that are the~~ most important. Interestingly, these
614 are regions where convective precipitation is particularly important for precipitation extremes. For wind extremes
615 downscaling effects also dominate, particularly over the British Isles, central Europe and the Alps. Results for TXx
616 and Rx5day are very similar to those for TXx5day and Rx1day respectively (not shown).

617
618 Also shown, using dashed lines, are the original ensemble mean results without using analogues. By comparing these
619 with the self-analogue results we can see how successful the analogue technique is in recreating the original
620 distributions. The self-analogue results tend to be close to the original results for wind and Rx1day, but below them
621 for Tx5day. Undertaking the 5-day ~~averaging-smoothing~~ first rather than last (see above) shifts analogue results
622 upwards, above the original curves, but the other aspects of the results are the same (not shown). A similar phenomenon
623 is seen for Rx5day (not shown).

624
625 In summary, for all three types of extreme events, downscaling effects appear to dominate the differences seen between
626 the 130km and 25km HadGEM3-A simulations. This suggests that at least for this model, any large scale circulation
627 differences obtained with global high resolution do not affect the statistics of these extreme events much.

628 **5 Discussion and Conclusions**

629 We evaluated climate model simulations of temperature, precipitation and wind extremes over Europe, addressing
630 three questions: 1) The benefits of dynamical downscaling using regional climate models by comparing EURO-
631 CORDEX simulations at two resolutions (12.5 and 50 km) to their driving coarser resolution CMIP5 models; 2) The
632 benefits of increased resolution for global models by comparing HadGEM3-A simulations at three resolutions (130,
633 60 and 25 km; referred to as the “UPSCALE” simulations); and 3) whether any differences according to resolution in
634 the global model comes from differences in the large scale circulation (upscaling) or the representation of small scale
635 processes, and features (downscaling) using a circulation analogue method.

636

637 For temperature extremes, increased resolution did not make much difference to results for the CORDEX vs CMIP5
638 analysis in terms of the shapes of the return period curves, which all agreed well with observational data. Hot biases
639 over mountains reduced with increased resolution, although the cold bias over Scandinavia was worse in CORDEX
640 than in CMIP5. This amplified Scandinavian cold bias in CORDEX is consistent with the findings of Sørland et al
641 (2018) for mean summer temperature, although we did not find the same reduction of the warm bias in Eastern Europe
642 in CORDEX as they did, possibly due to differences in the models used. Our findings agree with Vautard et al. (2013),
643 who find limited benefits in simulating various aspects of heatwaves between the 0.44° and 0.11° versions of the
644 EURO-CORDEX models. The reduction in orographic bias with increased resolution was also seen in the HadGEM3-
645 A GCM simulations, along with a general tendency towards hotter extremes elsewhere, which reduces biases in the
646 north, and increases them in the south. Overall the benefits of increasing resolution were limited, or region dependent.
647 However, our results for the global model analysis are based on only one model and the new model simulations and
648 analyses being generated as part of the PRIMAVERA and HighResMIP projects (<https://www.primavera-h2020.eu/>;
649 Roberts et al. 2018; Haarsma et al. 2016) will be very useful for determining how representative our results for
650 HadGEM3-A are of other GCMs. For instance, improvements in the simulation of summer blocking, which can be
651 involved in heatwave generation is very model dependent (Schieemann et al. 2014). Furthermore, Cattiaux et al.
652 (2013) find that the frequency, intensity and duration of summer heatwaves improve in the IPSL model with resolution,
653 associated with a better representation of the large scale circulation. In addition, here we examine only one aspect of
654 heat waves (intensity), and it could be that results are different for other aspects, such as frequency, duration and
655 timing.

656
657 Precipitation extremes were more sensitive to resolution, particularly in the CMIP5 vs CORDEX analysis, with heavier
658 tails at higher resolution across all regions. Spatially, CMIP5 shows a general dry bias compared to E-OBS, particularly
659 over mountainous regions, whilst CORDEX shows the opposite, with increasing wet differences at 0.11° compared to
660 0.44°, which appears to be systematic across models. This is consistent with results for mean precipitation in EURO-
661 CORDEX in Kotlarski et al. (2014). The higher resolution MESAN reanalysis gave wetter extremes and heavier tails
662 than E-OBS, agreeing best with the 0.44° resolution CORDEX simulations. Other studies suggest that country-scale
663 higher resolution precipitation datasets give heavier precipitation extremes still, which may agree best with the 0.11°
664 simulations (e.g. Prein and Gobiet 2017). Similarly, for mean precipitation, Prein and Gobeit (2017) find that RCM
665 biases are a similar size to the differences between different observational estimates. For extreme precipitation, various
666 studies find that a number of aspects (biases, frequency-intensity distributions, spatial patterns) of mean and extreme
667 precipitation improve in EURO-CORDEX at 0.11° compared to 0.44° when compared to such high resolution datasets
668 (e.g. Prein et al. 2016; Torma et al. 2015; Fantini et al. 2020). Prein et al (2016) ascribe this mostly to the better
669 representation of orography at higher resolution, but also the ability to capture the larger scales of convection.
670 However, aside from improved spatial patterns Casanueva et al (2016) found only limited evidence for improvements
671 in precipitation intensity, frequency and derived indicators over the Alps and Spain with resolution in EURO-
672 CORDEX. Some of the differences with resolution in our results may also be explained by parameterisation schemes
673 that tend to be tuned to one resolution and can behave sub-optimally at others.

674

675 For the UPSCALE global simulations, there was less difference in extreme precipitation with resolution, with the
676 biggest differences in southern regions or over or near mountains, with heavier tails and wetter extremes at higher
677 resolution. This reduced dry biases over orography, but wet biases next to some mountain ranges in the south emerged
678 instead. However, these simulations span a narrower range of resolutions, i.e. not reaching the same high resolutions
679 as CORDEX 0.11°, but also not as coarse as some CMIP5 models. Other global model studies also tend to find an
680 increase in precipitation extremes with increased resolution for Europe, which is continent-wide in summer, and
681 concentrated in mountainous regions in winter (Volosciuk et al. 2015; Wehner et al. 2014). This sometimes improves
682 agreement with observational data (e.g. Kopparla et al. 2013; Wehner et al. 2014 for winter), but can overestimate
683 summer extreme precipitation if parameterisation schemes are not retuned (Wehner et al. 2014).

684
685 For wind extremes, higher resolution gave somewhat stronger winds and heavier tails for most regions for both the
686 CORDEX vs CMIP5 analysis and to a lesser extent for HadGEM3-A, except for regions dominated by coasts for the
687 latter, where large coastal grid boxes at lower resolution brought strong ocean winds further over land. Stronger winds
688 with higher resolution are also found in previous studies (e.g. Pryor et al. 2012; Kunz et al. 2010; Gao et al. 2020). The
689 largest differences we found were between CMIP5 and CORDEX at 0.44°, with less difference between the two
690 resolutions of CORDEX. Differences between reanalysis-based estimates made model evaluation difficult.

691
692 The results of the circulation analogue analysis on the HadGEM3-A GCM simulations suggested that downscaling
693 effects were the dominant cause of differences with resolution for all three phenomena, with limited effects of any
694 differences in the representation of the large scale circulation. If this result also applied to other GCMs, it would suggest
695 that dynamical downscaling with more economical limited area models would be a better strategy for simulating
696 European extreme events, whilst GCM efforts could focus on other aspects such as multiple members or multi-physics
697 ensembles. However, we cannot reach this conclusion based solely on this analysis, since we examine only a single
698 model, which may not be representative of other models, and because the range of resolutions considered may be too
699 narrow. Demory et al. (2020) and Strandberg and Lind (2020) found that PRIMAVERA GCM simulations and EURO-
700 CORDEX simulations at comparable resolution simulated fairly similar precipitation PDFs to each other, which would
701 agree with a limited influence of upscaling. However, a number of studies do find improvements in the large-scale
702 circulation with resolution, including for extra-tropical cyclones and storm tracks (Colle et al. 2013; Jung et al 2006;
703 2012, Zappa et al. 2013), Euro-Atlantic weather regimes (Dawson et al. 2012; 2015; Cattiaux et al. 2013; Strommen
704 et al. 2019; Fabiano et al. 2020) and blocking (Jung et al. 2012, Anstey et al. 2013; Matsueda et al. 2009, Berckmans
705 et al 2013; Schei~~e~~mann et al. 2017; 2020; Davini et al 2017a; 2017b; 2020; see also Introduction). Interestingly,
706 Schei~~e~~mann et al. (2017) find improvements in Euro-Atlantic blocking with resolution in all seasons in the same
707 HadGEM3-A simulations as we analyse here. However, the net effects on extremes, given all uncertainties, was not
708 explicitly investigated. Our study does not seem to be able to discern such effects. Other studies suggest that benefits
709 from upscaling may require convective permitting simulations (Hart et al. 2018).

710
711 Overall our results suggest that whether or not increased resolution is beneficial for the simulation of extreme events
712 over Europe depends on the event being considered. Benefits appear limited for heatwaves, whereas wind extremes

713 and particularly precipitation extremes are more sensitive. We do not find any particular advantage in using a global
714 high resolution model compared to regional dynamical downscaling, with the caveats that this investigation needs to
715 be extended to other GCMs, and a wider range of resolutions should be investigated.

716
717 In order to fully address the question of the benefits of increased resolution for European climate extremes, a number
718 of aspects remain to be investigated. Firstly, the analysis could be widened to other types of extremes, for example,
719 sea level rise and storm surge, or other aspects of extremes could be considered e.g. timing, frequency and duration of
720 events. The global simulations we investigated were atmosphere-only, and the role of increased ocean resolution and
721 also vertical resolution and model top height should be considered. Finally, we assume that better historical
722 performance translates into more accurate future projections. Lhotka et al. (2018) find low sensitivity of heatwave
723 projections to resolution in EURO-CORDEX RCMs. However, Van Haren et al. (2015b) and van der Linden et al.
724 (2019) find stronger future summer drying and heating in central Europe with increased resolution in the EC-Earth
725 GCM due to differences in atmospheric circulation. Concerning precipitation, future projections for large scale and
726 seasonal mean precipitation are consistent between large scale regional and convective permitting models, whilst there
727 is evidence that summer sub-daily intensities increase more in the future in convection permitting models (Kendon et
728 al. 2014; 2017; Ban et al. 2015). For wind, Willison et al. (2015) find a larger response of the North Atlantic storm
729 track to global warming with higher resolution in the regional WRF model. Furthermore, Baker et al. (2019) find that
730 in winter the polar jet, storm tracks and associated precipitation shift further North over the Euro-Atlantic region in the
731 future with increased resolution in the same HadGEM3-A set up as used here. The sensitivity of projections to
732 resolution nevertheless remains an area that needs further research.

733
734 Finally, ongoing projects such as HighResMIP for CMIP6 (Haarsma et al., 2016), and the CORDEX Flagship Pilot
735 Studies, particularly the FPS on Convective Phenomena at High Resolution over Europe and the Mediterranean
736 (Coppola et al., 2019; Jacob et al 2020), will enable the benefits of high resolution and its effect on European climate
737 projections to be explored more thoroughly. The former will allow a systematic exploration of the effects of increased
738 resolution for multiple GCMs through coordinated experiments simulating the past and future climate. The latter will
739 include a first of its kind large multi-model ensemble at convective permitting resolution for decadal time slices in the
740 present and future for a large domain covering central Europe and part of the Mediterranean.

741 **Data and code availability**

742 The CMIP5 and CORDEX data used for this analysis are available from the Earth System Grid Federation portals, and
743 are detailed in Table S1. The HadGEM3-A UPSCALE simulations are available from the CEDA-JASMIN platform.
744 E-OBS can be downloaded here <https://www.ecad.eu/download/ensembles/download.php>, MESAN is available here
745 <http://exporter.nsc.liu.se/620eed0cb2c74c859f7d6db81742e114/>, ERA5 and MESCAN are available from the
746 Copernicus Climate Data Store <https://cds.climate.copernicus.eu>, whilst DYNAD winds are available from Tomas
747 Landelius at SMHI.

748 **Author contributions**

749 CI, RV and SJ conceptualised the study, CI carried out the analysis and wrote the manuscript, JS managed the CRECP
750 project together with CH and BE, and all co-authors were involved in discussions to prepare the study and helped
751 improve the manuscript.

752 **Competing interests**

753 The authors declare that they have no conflict of interest.

754 **Acknowledgements**

755 This work is published in the name of the European Commission, with funding from the European Union through the
756 Copernicus Climate Change Service project C3S_34a Lot 3 (Copernicus Roadmap for European Climate Projections).
757 The Commission is not responsible for any use that may be made of the information contained. We acknowledge the
758 WCRP's Working Group on Regional Climate, and the Working Group on Coupled Modelling - the coordinating body
759 of CORDEX and the panel responsible for CMIP5 respectively. We thank the climate modelling groups for producing
760 and making available the model output listed in Supplementary Table 1, which is available at <http://pcmdi9.llnl.gov>.
761 For CMIP, the US Department of Energy's Program for Climate Model Diagnosis and Intercomparison provides
762 coordinating support and led development of software infrastructure in partnership with the Global Organization for
763 Earth System Science Portals. We thank the modelling team that produced the UPSCALE simulations, and
764 acknowledge the JASMIN and IPSL mesocentre computing clusters on which this analysis was performed. We thank
765 Tomas Landelius from SMHI for making the DYNAD wind data available. We also acknowledge helpful input from
766 the CRECP project scientific advisory board and useful discussions with UK Met Office Scientists, in particular
767 Malcolm Roberts and Carol McSweeney. We thank four anonymous reviewers for their helpful comments and
768 suggestions.

770 **References**

771 Anstey, J. A., Davini, P., Gray, L. J., Woollings, T. J., Butchart, N., Cagnazzo, C., Christiansen, B., Hardiman, S. C.,
772 Osprey, S. M. and Yang, S.: Multi-model analysis of Northern Hemisphere winter blocking: Model biases and the role
773 of resolution, *J. Geophys. Res. Atmos.*, 118, 3956–3971, doi: 10.1002/jgrd.50231, 2013.

774
775 Bador, M., Boé, J., Terray, L., Alexander, L. V., Baker, A., Bellucci, A., Haarsma, R., Koenigk, T., Moine, M-P.,
776 Lohmann, K., Putrasahan, D. A., Roberts, C., Roberts, M., Scoccimarro, E., Schiemann, R., Seddon, J., Senan, R.,
777 Valcke, S., and Vanniere, B.: Impact of higher spatial atmospheric resolution on precipitation extremes over land in
778 global climate models. *J. Geophys. Res. Atmos.*, 125, e2019JD032184. <https://doi.org/10.1029/2019JD032184>, 2020

779

780 Baker, A.J., Schiemann, R., Hodges, K. I., Demory, M., Mizielinski, M. S., Roberts, M. J., Shaffrey, L. C., Strachan,
781 J. and Vidale, P. L.: Enhanced Climate Change Response of Wintertime North Atlantic Circulation, Cyclonic Activity,
782 and Precipitation in a 25-km-Resolution Global Atmospheric Model. *J. Climate*, 32, 7763–7781, [https://doi-](https://doi-org.ezproxy.is.ed.ac.uk/10.1175/JCLI-D-19-0054.1)
783 [org.ezproxy.is.ed.ac.uk/10.1175/JCLI-D-19-0054.1](https://doi-org.ezproxy.is.ed.ac.uk/10.1175/JCLI-D-19-0054.1), 2019

784

785 Ban, N., Schmidli, J. and Schär, C.: Heavy precipitation in a changing climate: Does short-term summer precipitation
786 increase faster?, *Geophys. Res. Lett.*, 42, 1165–1172, doi: 10.1002/2014GL062588, 2015.

787

788 Bazile, E., Abida, R., Verrelle, A., Le Moigne, P. and Szczypta, C. : Report for the 55years MESCAN-SURFEX re-
789 analysis, deliverable D2.8of the UERRA project, pp. 22, available from: [http://www.uerra.eu/publications/deliverable-](http://www.uerra.eu/publications/deliverable-reports.html)
790 [reports.html](http://www.uerra.eu/publications/deliverable-reports.html), 2017

791

792 Berckmans, J., Woollings, T., Demory, M. E., Vidale, P.-L. and Roberts, M.: Atmospheric blocking in a high resolution
793 climate model: influences of mean state, orography and eddy forcing, *Atmos. Sci. Lett.*, 14, 34–40,
794 doi:10.1002/asl2.412, 2013.

795

796 Casanueva, A., Kotlarski, S., Herrera, S., Fernández, J., Gutiérrez, J.M., Boberg, F., Colette, A., Christensen, O. B.,
797 Goergen, K., Jacob, D., Keuler, K., Nikulin, G., Teichmann C. and Vautard, R.: Daily precipitation statistics in a
798 EURO-CORDEX RCM ensemble: added value of raw and bias-corrected high-resolution simulations, *Clim Dynam*,
799 47,719-737. <https://doi.org/10.1007/s00382-015-2865-x>, 2016

800

801 Cattiaux, J., Vautard, R., Cassou, C., Yiou, P., Masson-Delmotte, V., and Codron, F.: Winter 2010 in Europe: A cold
802 extreme in a warming climate, *Geophys. Res. Lett.*, 37, L20704, doi: 10.1029/2010GL044613, 2010.

803

804 Cattiaux, J., Quesada, B., Arakélian, A., Codron, F., Vautard, R., Yiou, P.: North-Atlantic dynamics and European
805 temperature extremes in the IPSL model: sensitivity to atmospheric resolution, *Clim. Dynam.*, 40, 2293-2310,
806 doi:10.1007/s00382-012-1529-3, 2013.

807

808 Christensen, J. H. and Christensen, O. B.: A summary of the PRUDENCE model projections of changes in European
809 climate by the end of this century, *Climatic Change*, 81, 7–30, doi: 10.1007/s10584-006-9210-7, 2007.

810

811 Colle, B. A., Zhang, Z., Lombardo, K., Liu, P., Chang, E. and Zhang, M.: Historical evaluation and future prediction
812 in Eastern North America and western Atlantic extratropical cyclones in the CMIP5 models during the cool season, *J.*
813 *Climate.*, 26, 882–903, doi: 10.1175/JCLI-D-12-00498.1, 2013.

814

815 Coppola, E., Sobolowski, S., Pichelli, E., Raffaele, F., Ahrens, B., Anders, I., Ban, N., Bastin, S., Belda, M., Belusic,
816 D., Caldas-Alvarez, A., Margarida Cardos, R., Davolio, S., Dobler, A., Fernandez, J., Fita Borrell, L., Fumiere, Q.,

817 Giorgi, F., Goergen, K., Guettler, I., Halenka, T., Heinzeller, D., Hodnebrog, Ø., Jacob, D., Kartsios, S., Katragko, E.,
818 Kendon, E., Khodayar, S., Kunstmann, H., Knist, S., Lavín, A., Lind, P., Lorenz, T., Maraun, D., Marelle, L., van
819 Meijgaard, E., Milovac, J., Myhre, G., Panitz, H.-J., Piazza, M., Raffa, M., Raub, T., Rockel, B., Schär, C., Sieck, K.,
820 Soares, P. M. M., Somot, S., Srnec, L., Stocchi, P., Tölle, M., Truhetz, H., Vautard, R., de Vries, H. and Warrach-Sagi,
821 K.: A first-of-its-kind multi-model convection permitting ensemble for investigating convective phenomena over
822 Europe and the Mediterranean, *Clim. Dynam.*, 1-32, <https://doi.org/10.1007/s00382-018-4521-8>, 2018.

823

824 Dahlgren, P., Landelius, T., Kållberg, P. and Gollvik, S., A high-resolution regional reanalysis for Europe. Part 1:
825 Three-dimensional reanalysis with the regional High-Resolution Limited-Area Model (HIRLAM), *Q.J.R. Meteorol.*
826 *Soc.*, 142, 2119-2131, doi:10.1002/qj.2807, 2016

827

828 Davini, P., Corti, S., D'Andrea, F., Rivière, G., and von Hardenberg, J.: Improved Winter European Atmospheric
829 Blocking Frequencies in High-Resolution Global Climate Simulations. *J. Adv. Model. Earth Syst.*, 9, 2615–2634,
830 <https://doi.org/10.1002/2017MS001082>, 2017a.

831

832 Davini, P., von Hardenberg, J., Corti, S., Christensen, H. M., Juricke, S., Subramanian, A., Watson, P. A. G.,
833 Weisheimer, A., and Palmer, T. N.: Climate SPHINX: evaluating the impact of resolution and stochastic physics
834 parameterisations in the EC-Earth global climate model, *Geosci. Model Dev.*, 10, 1383-1402,
835 <https://doi.org/10.5194/gmd-10-1383-2017>, 2017b.

836

837 Davini, P., and D'Andrea, F.: From CMIP-3 to CMIP-6: Northern Hemisphere atmospheric blocking simulation in
838 present and future climate. *J. Climate*, doi: <https://doi.org/10.1175/JCLI-D-19-0862.1>, 2020

839

840 Dawson, A. and Palmer, T. N.: Simulating weather regimes: impact of model resolution and stochastic
841 parameterization. *Clim Dynam*, 44, 2177-2193, <https://doi.org/10.1007/s00382-014-2238-x>, 2015.

842

843 Dawson, A., Palmer, T. N., and Corti, S.: Simulating regime structures in weather and climate prediction models,
844 *Geophys. Res. Lett*, 39, L21805, <https://doi.org/10.1029/2012GL053284>, 2012.

845

846 Dee, D. P., Uppala, S. M., Simmons, A. J, Berrisford, P., Poli, P., Kobayashi, S., Andrae, U., Balmaseda, M. A.,
847 Balsamo, G., Bauer, P., Bechtold, P., Beljaars, A. C., van de Berg, L., Bidlot, J., Bormann, N., Delsol, C., Dragani, R.,
848 Fuentes, M., Geer, A. J., Haimberger, L., Healy, S. B., Hersbach, H., Hólm, E. V., Isaksen, L., Kållberg, P., Köhler,
849 M., Matricardi, M., McNally, A. P., Monge-Sanz, B. M., Morcrette, J., Park, B., Peubey, C., de Rosnay, P., Tavolato,
850 C., Thépaut, J. and Vitart, F.: The ERA-Interim reanalysis: Configuration and performance of the data assimilation
851 system, *Q. J. R. Meteorol. Soc.*, 137, 553–597, <https://doi.org/10.1002/qj.828>, 2011.

852

853 Demory, M. E., Vidale, P. L., Roberts, M. J., Berrisford, P., Strachan, J., Schiemann, R., and Mizielinski, M. S.: The
854 role of horizontal resolution in simulating drivers of the global hydrological cycle, *Clim. Dynam.*, 42, 2201–2225,
855 <https://doi.org/10.1007/s00382-013-1924-4>, 2014.

856

857 Demory, M.-E., Berthou, S., Sørland, S. L., Roberts, M. J., Beyerle, U., Seddon, J., Haarsma, R., Schär, C.,
858 Christensen, O. B., Fealy, R., Fernandez, J., Nikulin, G., Peano, D., Putrasahan, D., Roberts, C. D., Steger, C.,
859 Teichmann, C., and Vautard, R.: Can high-resolution GCMs reach the level of information provided by 12–50 km
860 CORDEX RCMs in terms of daily precipitation distribution?, *Geosci. Model Dev. Discuss.*,
861 <https://doi.org/10.5194/gmd-2019-370>, in review, 2020.

862

863 Donat M. G., Leckebusch G. C., Wild S., Ulbrich U.: Benefits and limitations of regional multi-model ensembles for
864 storm loss estimations, *Clim. Res.*, 44, 211–225. <https://doi.org/10.3354/cr00891>, 2010.

865

866 Donlon, C. J., Martin, M., Stark, J., Roberts-Jones, J., Fiedler, E., and Wimmer, W.: The Operational Sea Surface
867 Temperature and Sea Ice Analysis (OSTIA) system, *Remote Sens. Environ.*, 116, 140–158,
868 [doi:10.1016/j.rse.2010.10.017](https://doi.org/10.1016/j.rse.2010.10.017), 2012.

869

870 Eyring, V., Bony, S., Meehl, G. A., Senior, C. A., Stevens, B., Stouffer, R. J., and Taylor, K. E.: Overview of the
871 Coupled Model Intercomparison Project Phase 6 (CMIP6) experimental design and organization, *Geosci. Model Dev.*,
872 9, 1937–1958, <https://doi.org/10.5194/gmd-9-1937-2016>, 2016.

873

874 Fabiano, F., Christensen, H.M., Strommen, K., Athanasiadis, P., Baker, A., Schiemann, R. and Corti, S: Euro-Atlantic
875 weather Regimes in the PRIMAVERA coupled climate simulations: impact of resolution and mean state biases on
876 model performance. *Clim Dyn* 54, 5031–5048. <https://doi.org/10.1007/s00382-020-05271-w>, 2020

877

878 Fantini, A., Raffaele, F., Torma, C., Bacer, S., Coppola, E., Giorgi, F., Ahrens, B., Dubois, C., Sanchez, E. and
879 Verdecchia, M.: Assessment of multiple daily precipitation statistics in ERA-Interim driven Med-CORDEX and
880 EURO-CORDEX experiments against high resolution observations. *Clim Dyn* **51**, 877–900.
881 <https://doi.org/10.1007/s00382-016-3453-4>, 2018

882

883 Førland, E. and Institut, N. M.: Manual for Operational Correction of Nordic Precipitation Data. Norwegian
884 Meteorological Institute., 1996.

885

886 Gao, J., G., Shoshiro, M., Roberts, M. J., Haarsma, R., Putrasahan, D., Roberts, C. D., Scoccimarro, E., Terray, L.,
887 Vannière, B. and Vidale, P. L.: Influence of model resolution on bomb cyclones revealed by HighResMIP-
888 PRIMAVERA simulations, *Environ. Res. Lett.* 15, 084001, <https://doi.org/10.1088/1748-9326/ab88fa>, 2020

889

890 Giorgi F., Jones C., Asrar G. R.: Addressing climate information needs at the regional level: the CORDEX framework,
891 WMO Bull., 58:175–183, 2009.

892

893 Goodison, B. E., Louie, P. Y. and Yang, D.: The WMO solid precipitation measurement intercomparison. World
894 Meteorological Organization-Publications-WMO TD, Report No. 67, 65–70, 1997.

895

896 Gutjahr, O., Schefczyk, L., Reiter, P. and Heinemann, G.: Impact of the horizontal resolution on the simulation of
897 extremes in COSMO-CLM, Meteorol. Z., 25, 543 – 562, doi: 10.1127/metz/2016/0638, 2016.

898

899 Haarsma, R. J., Roberts, M. J., Vidale, P. L., Senior, C. A., Bellucci, A., Bao, Q., Chang, P., Corti, S., Fuckar, N. S.,
900 Guemas, V., von Hardenberg, J., Hazeleger, W., Kodama, C., Koenigk, T., Leung, L. R., Lu, J., Luo, J.-J., Mao, J.,
901 Mizielinski, M. S., Mizuta, R., Nobre, P., Satoh, M., Scoccimarro, E., Semmler, T., Small, J., and von Storch, J.-S.:
902 High Resolution Model Intercomparison Project (HighResMIP v1.0) for CMIP6, Geosci. Model Dev., 9, 4185-4208,
903 <https://doi.org/10.5194/gmd-9-4185-2016>, 2016.

904

905 Hart, N. C. G., Washington, R., and Stratton, R. A.: Stronger local overturning in convective-permitting regional
906 climate model improves simulation of the subtropical annual cycle. Geophys. Res. Lett., 45, 11334–11342,
907 <https://doi.org/10.1029/2018GL079563>, 2018.

908

909 Haylock, M. R., Hofstra, N., Klein Tank, A. M. G., Klok, E. J., Jones, P. D., New, M.: A European daily high-resolution
910 gridded data set of surface temperature and precipitation for 1950-2006. J. Geophys. Res. Atmos., 113, D20119.
911 doi:10.1029/2008JD010201, 2008.

912

913 Herrera, S., Cardoso, R. M., Soares, P. M., Espírito-Santo, F., Viterbo, P., and Gutiérrez, J. M.: Iberia01: a new gridded
914 dataset of daily precipitation and temperatures over Iberia, Earth Syst. Sci. Data, 11, 1947–1956,
915 <https://doi.org/10.5194/essd-11-1947-2019>, 2019.

916

917 Herrmann, M., Somot, S., Calmanti, S., Dubois, C., and Sevault, F.: Representation of spatial and temporal variability
918 of daily wind speed and of intense wind events over the Mediterranean Sea using dynamical downscaling: impact of
919 the regional climate model configuration, Nat. Hazards Earth Syst. Sci., 11, 1983-2001, [https://doi.org/10.5194/nhess-](https://doi.org/10.5194/nhess-11-1983-2011)
920 11-1983-2011, 2011.

921

922 Hersbach, H., Bell, B., Berrisford, P., Horányi, A., Muñoz-Sabater, J., Nicolas, J., Radu, R., Schepers, D., Simmons,
923 A., Soci, C., Dee, D.: Global reanalysis: goodbye ERA-Interim, hello ERA5. ECMWF, doi:10.21957/vf291hehd7.
924 <https://www.ecmwf.int/node/19027>, 2019

925

926 Jacob, D., Petersen, J., Eggert, B., Alias, A., Christensen, O. B., Bouwer, L. M., Braun, A., Colette, A., Déqué, M.,
927 Georgievski, G., Georgopoulou, E., Gobiet, A., Menut, L., Nikulin, G., Haensler, A., Hempelmann, N., Jones, C.,

928 Keuler, K., Ko-vats, S., Kröner, N., Kotlarski, S., Kriegsman, A., Martin, E., Meijgaard, E. van, Moseley, C., Pfeifer,
929 S., Preuschmann, S., Radermacher, C., Radtke, K., Rechid, D., Rounsevell, M., Samuelsson, P., Somot, S., Soussana,
930 J.-F., Teichmann, C., Valentini, R., Vautard, R., Weber, B., and Yiou, P.: EURO-CORDEX: new high-resolution
931 climate change projections for European impact research, *Reg. Environ. Change*, 14, 563–578, doi:10.1007/s10113-
932 013-0499-2, 2014.

933

934 Jacob, D., Teichmann, C., Sobolowski, S. *et al.* Regional climate downscaling over Europe: perspectives from the
935 EURO-CORDEX community. *Reg Environ Change*, **20**, 51, <https://doi.org/10.1007/s10113-020-01606-9>, 2020

936

937 Jézéquel, A., Yiou, P. and Radanovics, S.: Role of circulation in European heatwaves using flow analogues. *Clim.*
938 *Dynam.* 50, 1145-1159, <https://doi.org/10.1007/s00382-017-3667-0>, 2018.

939

940 Jourdier, B.: Evaluation of ERA5, MERRA-2, COSMO-REA6, NEWA and AROME to simulate wind power
941 production over France, *Adv. Sci. Res.*, 17, 63–77, <https://doi.org/10.5194/asr-17-63-2020>, 2020.

942

943 Jung, T., Gulev, S. K., Rudeva, I. and Soloviov, V.: Sensitivity of extratropical cyclone characteristics to horizontal
944 resolution in the ECMWF model. *Q.J.R. Meteorol. Soc.*, 132, 1839-1857, doi:10.1256/qj.05.212, 2006.

945

946 Jung, T., Miller, M. J., Palmer, T. N., Towers, P., Wedi, N., Achuthavarier, D., Adams, J. M., Alshuler, E. L., Cash,
947 B. A., Kinter, J. L., Marx, L., Stan, C., and Hodges, K. I.: High-Resolution Global Climate Simulations with the
948 ECMWF Model in Project Athena: Experimental Design, Model Climate, and Seasonal Forecast Skill, *J. Climate.*, 25,
949 3155–3172, doi:10.1175/JCLI-D-11-00265.1, 2012.

950

951 Kendon, E. J., Roberts, N. M., Senior, C. A., and Roberts, M. J.: Realism of rainfall in a very high-resolution regional
952 climate model, *J. Climate.*, 25, 5791–5806. doi: 10.1175/JCLI-D-11-00562.1, 2012.

953

954 Kendon, E. J., Roberts, N. M., Fowler, H. J., Roberts, M. J., Chan, S. C., and Senior, C. A.: Heavier summer downpours
955 with climate change revealed by weather forecast resolution model, *Nat. Clim. Change*, 4, 570–576, doi:
956 10.1038/nclimate2258, 2014.

957

958 Kendon, E. J., Ban, N., Roberts, N. M., Fowler, H. J., Roberts, M. J., Chan, S. C., Evans, J. P., Fosser, G. and
959 Wilkinson, J.M.: Do Convection-Permitting Regional Climate Models Improve Projections of Future Precipitation
960 Change?. *B. Am. Meteorol. Soc.*, 98, 79–93, <https://doi.org/10.1175/BAMS-D-15-0004.1>, 2017.

961

962 Klaver, R., Haarsma, R., Vidale, P. L., Hazeleger, W.: Effective resolution in high resolution global atmospheric
963 models for climate studies. *Atmos Sci Lett.*, 1– 8. <https://doi.org/10.1002/asl.952>, 2020

964

965 Kopparla, P., Fischer, E. M., Hannay, C., and Knutti, R.: Improved simulation of extreme precipitation in a high-
966 resolution atmosphere model, *Geophys. Res. Lett.*, 40, 5803-5808, doi: 10.1002/2013GL057866, 2013.
967

968 Kotlarski, S., Keuler, K., Christensen, O. B., Colette, A., Déqué, M., Gobiet, A., Goergen, K., Jacob, D., Lüthi, D.,
969 van Meijgaard, E., Nikulin, G., Schär, C., Teichmann, C., Vautard, R., Warrach-Sagi, K., and Wulfmeyer, V.: Regional
970 climate modeling on European scales: a joint standard evaluation of the EURO-CORDEX RCM ensemble, *Geosci.
971 Model Dev.*, 7, 1297–1333, <https://doi.org/10.5194/gmd-7-1297-2014>, 2014.
972

973 Kunz, M., Mohr, S., Rauthe, M., Lux, R., and Kottmeier, C.: Assessment of extreme wind speeds from Regional
974 Climate Models – Part 1: Estimation of return values and their evaluation, *Nat. Hazards Earth Syst. Sci.*, 10, 907-922,
975 <https://doi.org/10.5194/nhess-10-907-2010>, 2010.
976

977 Landelius, T., Dahlgren, P., Gollvik, S., Jansson, A. and Olsson, E.: A high-resolution regional reanalysis for Europe.
978 Part 2: 2D analysis of surface temperature, precipitation and wind, *Q. J. R. Meteorol. Soc.*, 142, 2132–2142,
979 doi:10.1002/qj.2813, 2016.
980

981 Lhotka, O., Kysely, J. and Farda, A.: Climate change scenarios of heat waves in Central Europe and their uncertainties.
982 *Theor Appl Climatol.*, 131, 1043-1054, <https://doi.org/10.1007/s00704-016-2031-3>, 2018.
983

984 Matsueda, M., Mizuta, R. and Kusunoki, S.: Future change in wintertime atmospheric blocking simulated using a 20-
985 km-mesh atmospheric global circulation model, *J. Geophys. Res.*, 114, D12114, doi: 10.1029/2009JD011919, 2009.
986

987 Mizielinski, M. S., Roberts, M. J., Vidale, P. L., Schiemann, R., Demory, M.-E., Strachan, J., Edwards, T., Stephens,
988 A., Lawrence, B. N., Pritchard, M., Chiu, P., Iwi, A., Churchill, J., del Cano Novales, C., Kettleborough, J., Roseblade,
989 W., Selwood, P., Foster, M., Glover, M., and Malcolm, A.: High-resolution global climate modelling: the UPSCALE
990 project, a large-simulation campaign, *Geosci. Model Dev.*, 7, 1629–1640, doi:10.5194/gmd-7-1629-2014, 2014.
991

992 Niermann, D., Kaiser-Weiss, A., Borsche, M., van den Besselaar, E., Lussana, C., Isotta, F., Frei, C., Cantarello, L.,
993 Tveito, O. E., van der Schrier, G., Cornes, R., Vreede, E., Bojariu, R., and Davie, J.: Report for Deliverable 3.6 of the
994 UERRA project: Scientific report on assessment of regional analysis against independent data sets, pp. 138 , available
995 from: <http://www.uerra.eu/publications/deliverable-reports.html>
996

997 O'Brien, T. A., Collins, W. D., Kashinath, K., Rübel, O., Byna, S., Gu, J., Krishnan, H. and Ullrich, P. A.: Resolution
998 dependence of precipitation statistical fidelity in hindcast simulations, *J. Adv. Model. Earth Syst.*, 8, 976–990, doi:
999 10.1002/2016MS000671, 2016.
1000

1001 O'Reilly, C. H., Minobe, S. and Kuwano-Yoshida, A.: The influence of the Gulf Stream on wintertime European
1002 blocking, *Clim. Dynam.*, 47, 1545- 1567, <https://doi.org/10.1007/s00382-015-2919-0>, 2016.

1003
1004 Prein, A. F. and Gobiet, A.: Impacts of uncertainties in European gridded precipitation observations on regional climate
1005 analysis, *Int. J. Climatol.*, 37, 305-327, doi:10.1002/joc.4706, 2017.
1006
1007 Prein, A. F., Langhans, W., Fossier, G., Ferrone, A., Ban, N., Goergen, K., Keller, M., Tölle, M., Gutjahr, O., Feser,
1008 F., Brisson, E., Kollet, S., Schmidli, J., Van Lipzig, N. P. M., and Leung, R.: A review on regional convection-
1009 permitting climate modeling: Demonstrations, prospects, and challenges, *Rev. Geophys.*, 53, 323–361. doi:
1010 10.1002/2014RG000475, 2015.
1011
1012 Prein, A.F., Gobiet, A., Truhetz, H., Keuler, K., Goergen, K., Teichmann, C., Fox Maule, C., van Meijgaard, E., Déqué,
1013 M., Nikulin, G., Vautard, R., Colette, A., Kjellström, E., and Jacob, D.: Precipitation in the EURO-CORDEX 0.11°
1014 and 0.44° simulations: high resolution, high benefits?, *Clim. Dynam.* 46, 383-412, doi: 10.1007/s00382-015-2589-y,
1015 2016.
1016
1017 Pryor, S. C., Nikulin, G., and Jones, C.: Influence of spatial resolution on regional climate model derived wind climates,
1018 *J. Geophys. Res.*, 117, D03117, doi:10.1029/2011JD016822, 2012
1019
1020 Risanto, C.B., Castro, C.L., Moker, J.M., Jr., Arellano, A.F., Jr., Adams, D.K., Fierro, L.M., Minjarez Sosa, C.M.:
1021 Evaluating Forecast Skills of Moisture from Convective-Permitting WRF-ARW Model during 2017 North
1022 American Monsoon Season. *Atmosphere*, 10, 694, doi:[10.3390/atmos10110694](https://doi.org/10.3390/atmos10110694), 2019
1023
1024 Roberts, M. J., Vidale, P. L., Senior, C., Hewitt, H. T., Bates, C., Berthou, S., Chang, P., Christensen, H. M., Danilov,
1025 S., Demory, M. E., Griffies, S. M., Haarsma, R., Jung, T., Martin, G., Minobe, S., Ringler, T., Satoh, M., Schiemann,
1026 R., Scoccimarro, E., Stephens, G. and Wehner, M.F.: The benefits of global high-resolution for climate simulation:
1027 process-understanding and the enabling of stakeholder decisions at the regional scale.. *B. Am. Meteorol. Soc.*, 99,
1028 2341–2359 <https://doi.org/10.1175/BAMS-D-15-00320.1>, 2018.
1029
1030 Ruti, P. M., Somot, S., Giorgi, F., Dubois, C., Flaounas, E., Obermann, A., Dell’Aquila, A., Pisacane, G., Harzallah,
1031 A., Lombardi, E., Ahrens, B., Akhtar, N., Alias, A., Arsouze, T., Aznar, R., Bastin, S., Bartholy, J., Béranger, K.,
1032 Beuvier, J., Bouffies-Cloch e, S., Brauch, J., Cabos, W., Calmanti, S., Calvet, J., Carillo, A., Conte, D., Coppola, E.,
1033 Djurdjevic, V., Drobinski, P., Elizalde-Arellano, A., Gaertner, M., Gal n, P., Gallardo, C., Gualdi, S., Goncalves, M.,
1034 Jorba, O., Jord , G., L’Heveder, B., Lebeaupin-Brossier, C., Li, L., Liguori, G., Lionello, P., Maci s, D., Nabat, P.,
1035  nol, B., Raikovic, B., Ramage, K., Sevault, F., Sannino, G., Struglia, M. V., Sanna, A., Torma, C., and Vervatis, V.:
1036 Med-CORDEX Initiative for Mediterranean Climate Studies. *B. Am. Meteorol. Soc.*, 97, 1187–1208,
1037 <https://doi.org/10.1175/BAMS-D-14-00176.1>, 2016
1038

1039 Schiemann, R., Demory, M. E., Shaffrey, L. C., Strachan, J., Vidale, P. L., Mizielinski, M. S., Roberts, M. J., Matsueda,
1040 M., Wehner, M. F. and Jung, T.: The resolution sensitivity of Northern Hemisphere blocking in four 25-km
1041 atmospheric global circulation models, *J. Climate.*, 30, 337–358, <https://doi.org/10.1175/JCLI-D-16-0100.1>, 2017.
1042

1043 Schiemann, R., Vidale, P. L., Shaffrey, L. C., Johnson, S. J., Roberts, M. J., Demory, M.-E., Mizielinski, M. S., and
1044 Strachan, J.: Mean and extreme precipitation over European river basins better simulated in a 25 km AGCM, *Hydrol.*
1045 *Earth Syst. Sci.*, 22, 3933-3950, <https://doi.org/10.5194/hess-22-3933-2018>, 2018.
1046

1047 Schiemann, R., Athanasiadis, P., Barriopedro, D., Doblas-Reyes, F., Lohmann, K., Roberts, M. J., Sein, D. V., Roberts,
1048 C. D., Terray, L., and Vidale, P. L.: Northern Hemisphere blocking simulation in current climate models: evaluating
1049 progress from the Climate Model Intercomparison Project Phase 5 to 6 and sensitivity to resolution, *Weather Clim.*
1050 *Dynam.*, 1, 277–292, <https://doi.org/10.5194/wcd-1-277-2020>, 2020.
1051

1052 Seneviratne, S. I., Nicholls, N., Easterling, D., Goodess, C. M., Kanae, S., Kossin, J., Luo, Y., Marengo, J., McInnes,
1053 K., Rahimi, M., Reichstein, M., Sorteberg, A., Vera, C. and Zhang, X.: Changes in climate extremes and their impacts
1054 on the natural physical environment. In: *Managing the Risks of Extreme Events and Disasters to Advance Climate*
1055 *Change Adaptation. A Special Report of Working Groups I and II of the Intergovernmental Panel on Climate Change*,
1056 edited by: Field, C. B., Barros, V., Stocker, T. F., Qin, D., Dokken, D. J., Ebi, K., L. Mastrandrea, M. D., Mach, K.
1057 J., Plattner, G.-K., Allen, S. K., Tignor, M. and Midgley, P. M., Cambridge University Press, Cambridge, UK, and
1058 New York, NY, USA, pp. 109-230, 2012
1059

1060 Shields, C. A., Kiehl, J. T., and Meehl, G. A.: Future changes in regional precipitation simulated by a half-degree
1061 coupled climate model: Sensitivity to horizontal resolution, *J. Adv. Model. Earth Syst.*, 8, 863–884, doi:
1062 10.1002/2015MS000584, 2016.
1063

1064 Skamarock, W.C.: Evaluating Mesoscale NWP Models Using Kinetic Energy Spectra. *Mon. Wea. Rev.*, 132, 3019–
1065 3032, <https://doi.org/10.1175/MWR2830.1>, 2004
1066

1067 Strandberg, G. and Lind, P.: The importance of model resolution on simulated precipitation in Europe – from global
1068 to regional model, *Weather Clim. Dynam. Discuss.*, <https://doi.org/10.5194/wcd-2020-31>, in review, 2020.
1069

1070 Stott, P. A., Christidis, N., Otto, F. E., Sun, Y., Vanderlinden, J., van Oldenborgh, G. J., Vautard, R., von Storch, H.,
1071 Walton, P., Yiou, P. and Zwiers, F. W.: Attribution of extreme weather and climate-related events. *WIREs Clim.*
1072 *Change*, 7, 23-41. doi:10.1002/wcc.380, 2016.
1073

1074 Strommen, K., Mavilia, I., Corti, S., Matsueda, M., Davini, P., von Hardenberg, J., Vidale, P.-L. and Mizuta, R. : The
1075 sensitivity of Euro-Atlantic regimes to model horizontal resolution. *Geophysical Research*
1076 *Letters*, 46, 7810– 7818. <https://doi.org/10.1029/2019GL082843>, 2019

1077
1078 Taylor, K., Williamson, D., and Zwiers, F.: The sea surface temperature and sea-ice concentration boundary conditions
1079 for AMIP II simulations, PCMDI Rep. 60, Tech. Rep. 60, PCMDI, 25 pp., available at: [http://www-](http://www-pcmdi.llnl.gov/publications/ab60.html)
1080 [pcmdi.llnl.gov/publications/ab60.html](http://www-pcmdi.llnl.gov/publications/ab60.html), 2000.
1081
1082 Taylor, K. E., Stouffer, R. J. and Meehl, G. A.: An overview of CMIP5 and the experiment design, *B. Am. Meteorol.*
1083 *Soc.*, 93, 485498, doi: 10.1175/BAMS-D-11-00094.1, 2012.
1084
1085 Terai, C. R., Caldwell, P. M., Klein, S. A. Tang, Q. and Branstetter, M. L.: The atmospheric hydrologic cycle in the
1086 ACME v0.3 model. *Clim. Dynam.*, 50, 3251- 3279. <https://doi.org/10.1007/s00382-017-3803-x>, 2018.
1087
1088 Torma, C., Giorgi, F. and Coppola, E.: Added value of regional climate modeling over areas characterized by complex
1089 terrain—Precipitation over the Alps, *J. Geophys. Res. Atmos.*, 120, 3957–3972, doi: 10.1002/2014JD022781, 2015.
1090
1091 van der Linden, E. C., Haarsma, R. J., and van der Schrier, G.: Impact of climate model resolution on soil moisture
1092 projections in central-western Europe, *Hydrol. Earth Syst. Sci.*, 23, 191–206, [https://doi.org/10.5194/hess-23-191-](https://doi.org/10.5194/hess-23-191-2019)
1093 2019, 2019.
1094
1095 Van Haren, R., Haarsma, R. J., Van Oldenborgh, G. J. and Hazeleger, W.: Resolution Dependence of European
1096 Precipitation in a State-of-the-Art Atmospheric General Circulation Model, *J. Climate.*, 28, 5134–5149, doi:
1097 10.1175/JCLI-D-14-00279.1, 2015a.
1098
1099 Van Haren, R., Haarsma, R. J., de Vries, H., van Oldenborgh, G. J., and Hazeleger, W.: Resolution dependence of
1100 circulation forced future central European summer drying, *Environ. Res. Lett.*, 10, 055002, doi:10.1088/1748-
1101 9326/10/5/055002, 2015b.
1102
1103 Vanniere, B., Vidale, P. L., Demory, M.-E., Schiemann, R., Roberts, M. J., Roberts, C. D., Matsueda, M., Terray, L.,
1104 Koenigk, T., Senan, R.: Multi-model evaluation of the sensitivity of the global energy budget and hydrological cycle
1105 to resolution, *Clim. Dynam.*, 52, 6817- 6846, <https://doi.org/10.1007/s00382-018-4547-y>, 2019
1106
1107 Vautard, R., Gobiet, A., Jacob, D., Belda, M., Colette, A., Déqué, M., Fernández, J., García-Díez, M., Goergen, K.,
1108 Güttler, I., Halenka, T., Karacostas, T., Katragkou, E., Keuler, K., Kotlarski, S., Mayer, S., van Meijgaard, E., Nikulin,
1109 G., Patarcic, M., Scinocca, J., Sobolowski, S., Suklitsch, M., Teichmann, C., Warrach-Sagi, K., Wulfmeyer, V., Yiou,
1110 P. : The simulation of European heat waves from an ensemble of regional climate models within the EURO-CORDEX
1111 project, *Clim. Dynam.*, 41, 2555-2575, doi: 10.1007/s00382-013-1714-z, 2013.
1112

1113 Vautard, R., Yiou, P., Otto, F., Stott, P., Christidis, N., van Oldenborgh, G. J. and Schaller, N.: Attribution of human-
1114 induced dynamical and thermodynamical contributions in extreme weather events, *Environ. Res. Lett.*, 11, 114009,
1115 <https://doi.org/10.1088/1748-9326/11/11/114009>, 2016.
1116

1117 Volosciuk, C., Maraun, D., Semenov, V.A. and Park, W.: Extreme Precipitation in an Atmosphere General Circulation
1118 Model: Impact of Horizontal and Vertical Model Resolutions, *J. Climate.*, 28, 1184–1205,
1119 <https://doi.org/10.1175/JCLI-D-14-00337.1>, 2015.
1120

1121 Vries, H. de, Scher, S., Haarsma, R., Drijfhout, S., and Delden, A. van.: How Gulf-Stream SST-fronts influence
1122 Atlantic winter storms, *Clim. Dynam.*, 52, 5899-5909. <https://doi.org/10.1007/s00382-018-4486-7>, 2019
1123

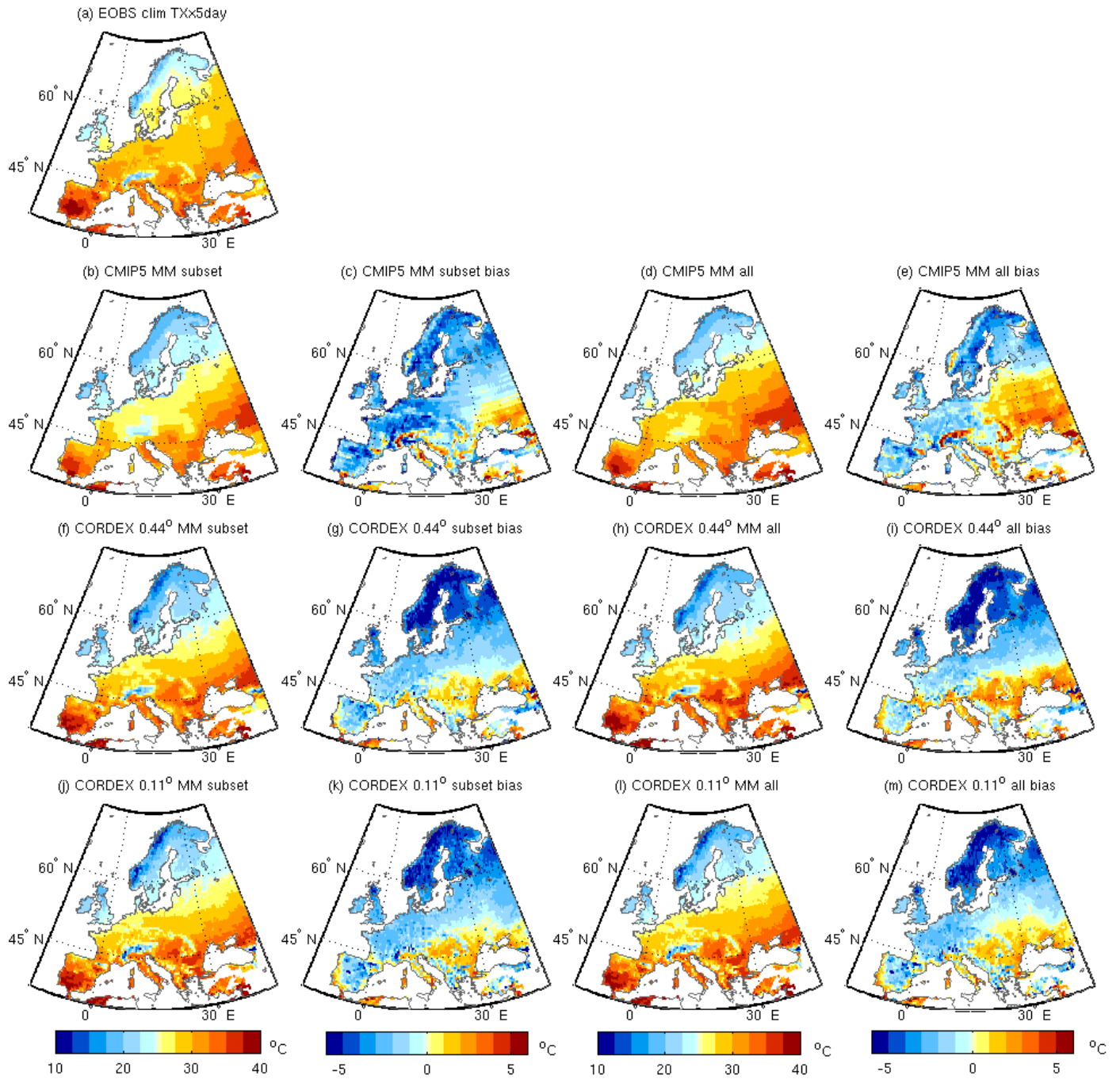
1124 Wehner, M. F., Smith, R. L., Bala, G. and Duffy, P.: The effect of horizontal resolution on simulation of very extreme
1125 US precipitation events in a global atmosphere model, *Clim. Dynam.*, 34, 241-247. [https://doi.org/10.1007/s00382-](https://doi.org/10.1007/s00382-009-0656-y)
1126 [009-0656-y](https://doi.org/10.1007/s00382-009-0656-y), 2010.
1127

1128 Wehner, M. F., Reed, K. A., Li, F., Prabhat, Bacmeister, J., Chen, C.-T., Paciorek, C., Gleckler, P. J., Sperber, K. R.,
1129 Collins, W. D., Gettelman, A., and Jablonowski, C.: The effect of horizontal resolution on simulation quality in the
1130 Community Atmospheric Model, CAM5.1, *J. Adv. Model. Earth Syst.*, 6, 980–997, doi:10.1002/2013MS000276,
1131 2014.
1132

1133 Willison, J., Robinson, W.A. and Lackmann, G.M.: North Atlantic Storm-Track Sensitivity to Warming Increases with
1134 Model Resolution., *J. Climate.*, 28, 4513–4524, <https://doi.org/10.1175/JCLI-D-14-00715.1>, 2015.
1135

1136 Zappa, G., Shaffrey, L. C. and Hodges, K. I., The Ability of CMIP5 Models to Simulate North Atlantic Extratropical
1137 Cyclones, *J. Climate.*, 26, 5379-5396, doi: 10.1175/JCLI-D-12-00501.1, 2013.
1138

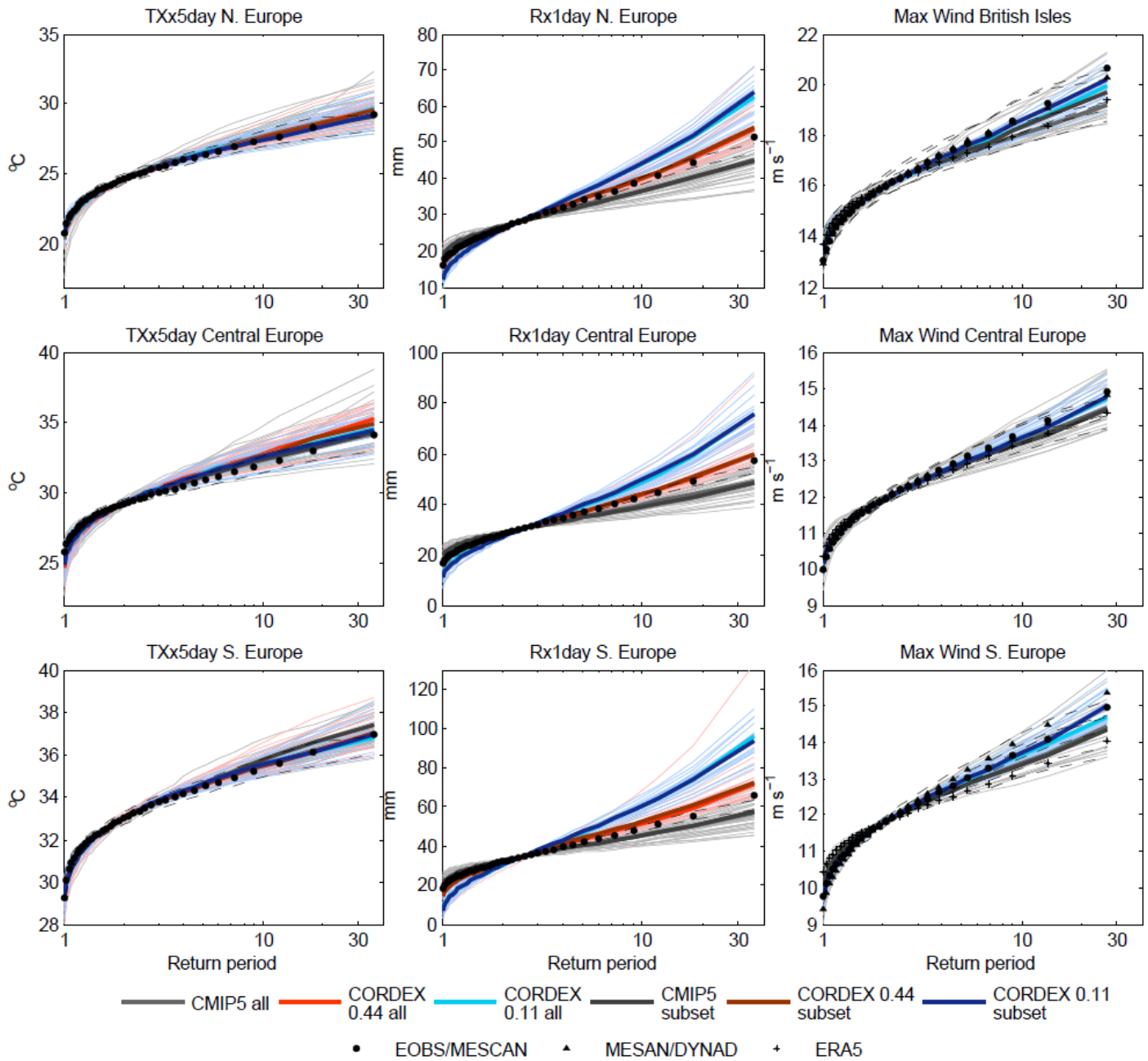
1139 Zhang, X., Alexander, L., Hegerl, G. C., Jones, P., Tank, A. K., Peterson, T. C. Trewin, B. and Zwiers, F. W.: Indices
1140 for monitoring changes in extremes based on daily temperature and precipitation data, *Wiley Interdiscip. Rev., Clim.*
1141 *Chang.*, 2, 851–870, doi:10.1002/wcc.147, 2011.
1142



1144

1145 **Figure 1: Climatological mean of TXx5day for the period 1970-2005 for (a) E-OBS; the multi model median of the common**
 1146 **subset of models (see Methods) for (b) CMIP5, (f) CORDEX 0.44° and (j) CORDEX 0.11°, (c, g, k) their biases with respect**
 1147 **to E-OBS, and (d,e,h,i,j,k) the same for the full ensembles of CMIP5 and CORDEX. Units °C.**

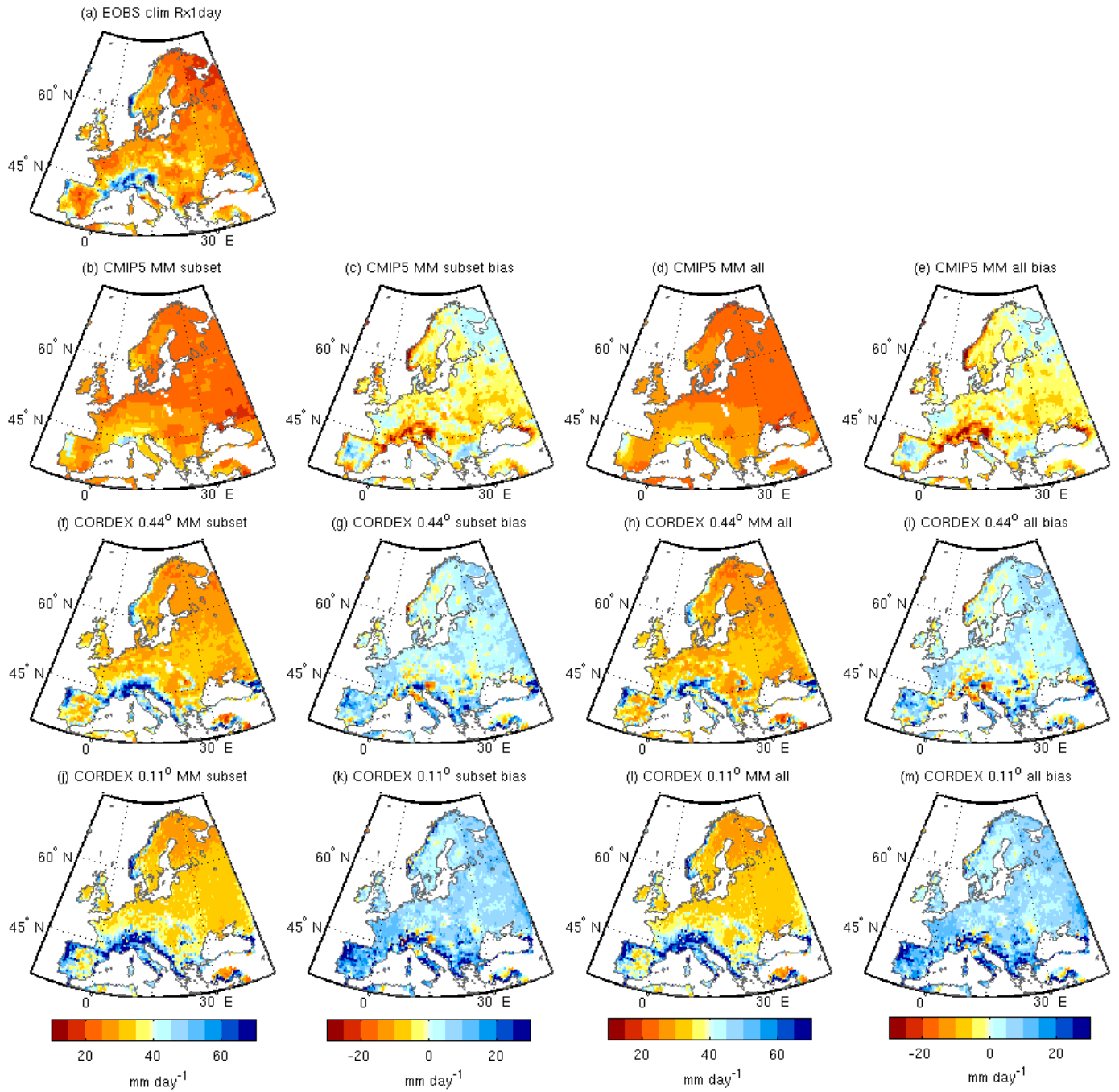
1148



1149

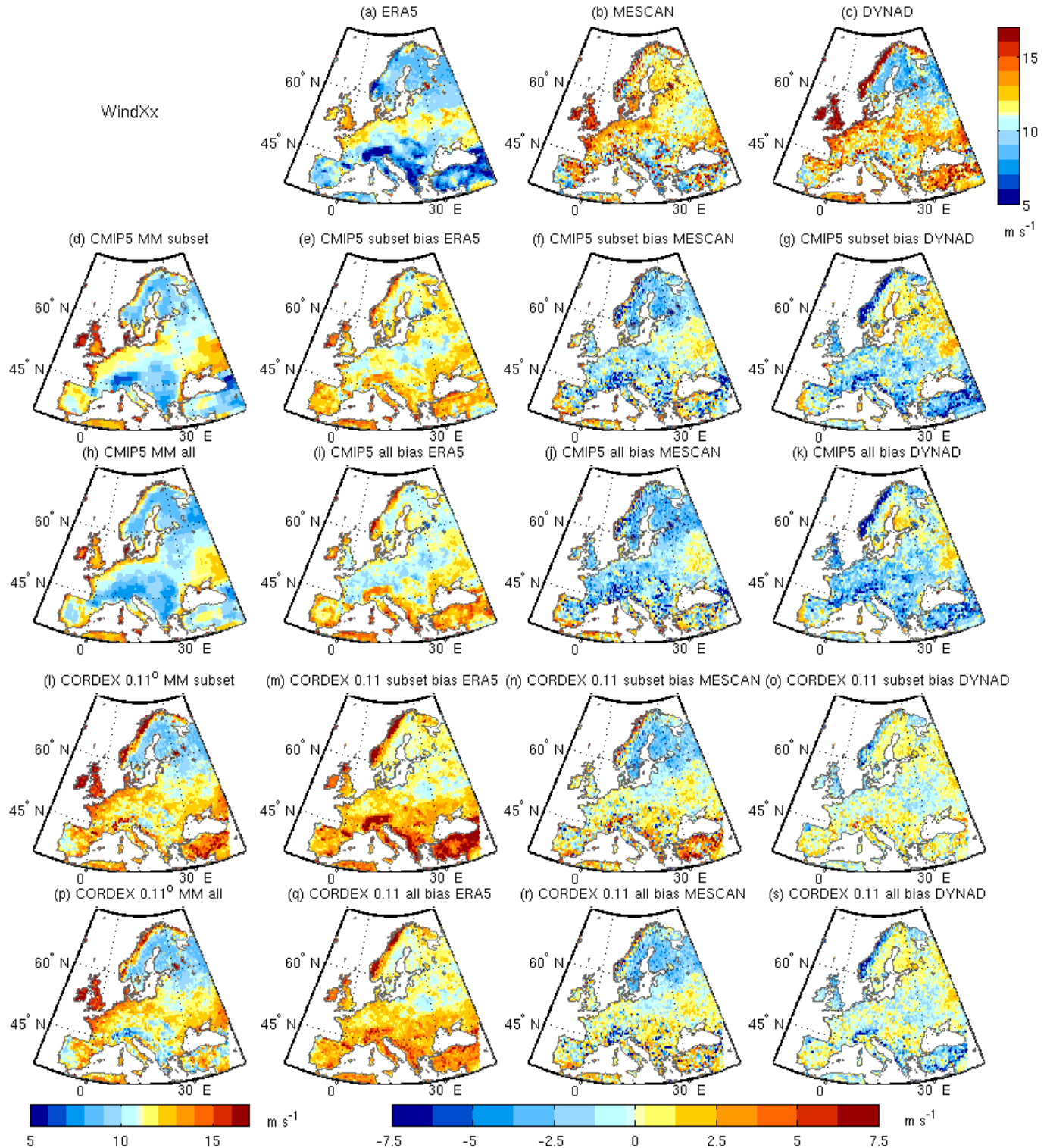
1150 **Figure 2: Return period plots for (left) TXx5day, (middle column) Rx1day and (right) annual maximum wind, for CMIP5**
 1151 **and CORDEX for Northern Europe (top row (except top right = British Isles)), Central Europe (middle row) and Southern**
 1152 **Europe (bottom row). CMIP5 is shown in grey, CORDEX 0.44° in red and CORDEX 0.11° in blue. Thin lines are individual**
 1153 **ensemble members, thick lines are multi model medians: lighter colours for the full ensembles, and darker colours for the**
 1154 **subset of models common to CMIP5 and both CORDEX resolutions. Observational datasets are shown in black, circles for**
 1155 **E-OBS temperature and precipitation and MESCAN wind, triangles for MESAN precipitation and DYNAD wind and**
 1156 **crosses for ERA5 wind. Confidence intervals based on bootstrapping are shown with dashed lines for the observational**
 1157 **datasets. The time periods considered are 1970-2005 for TXx5day and Rx1day, and 1979-2005 for wind.**

1158



1159

1160 **Figure 3: As for Figure 1 but for the climatological mean of Rx1day. Units mm.**



1161
 1162 **Figure 4: Climatological mean of annual maximum wind for the period 1979-2005 for (a) ERA5, (b) MESCAN (c)**
 1163 **DYNAD, and for the multi model median of the common subset of models for (d) CMIP5 and (l) CORDEX 0.11° and their**
 1164 **biases with respect to the reanalyses datasets (e-g and m-o). (h-k and p-s) are the same but for the full ensembles of**
 1165 **CMIP5 and CORDEX. Units meters per second.**

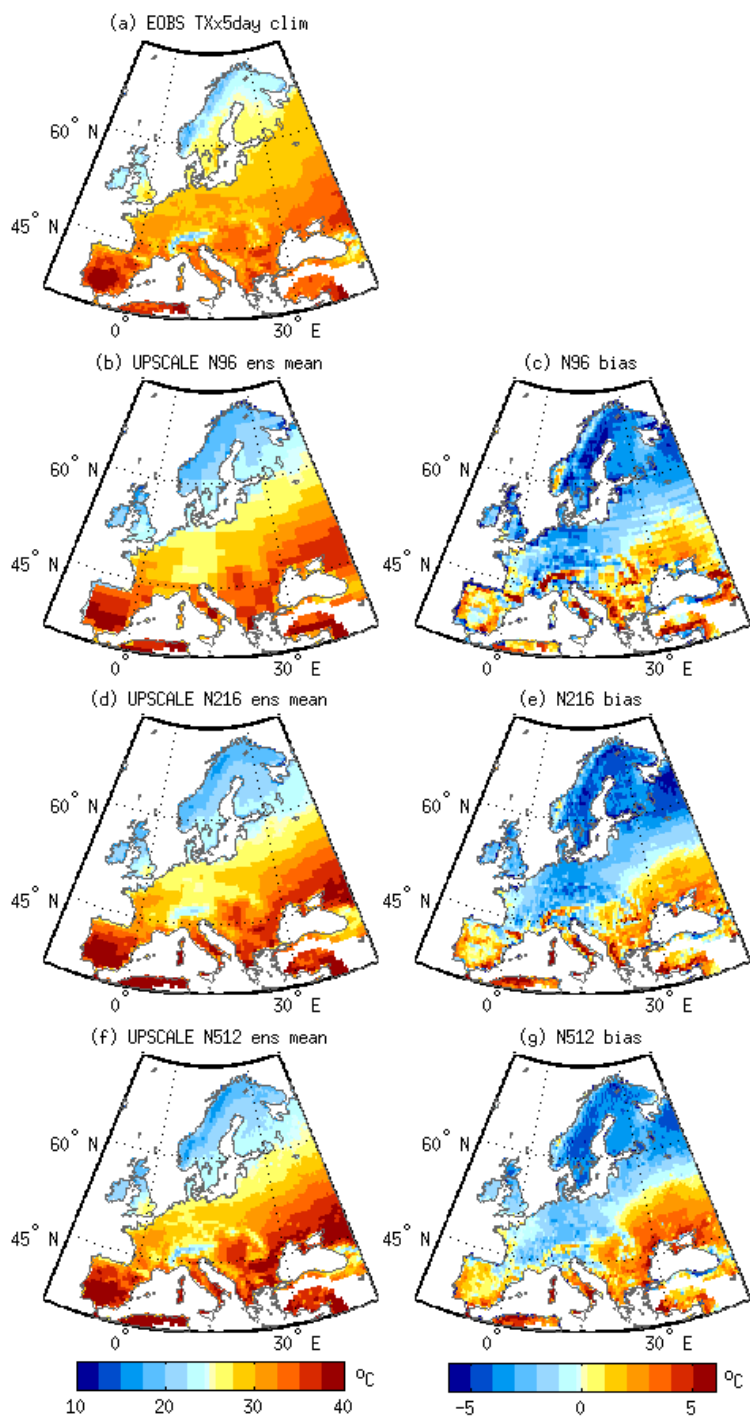
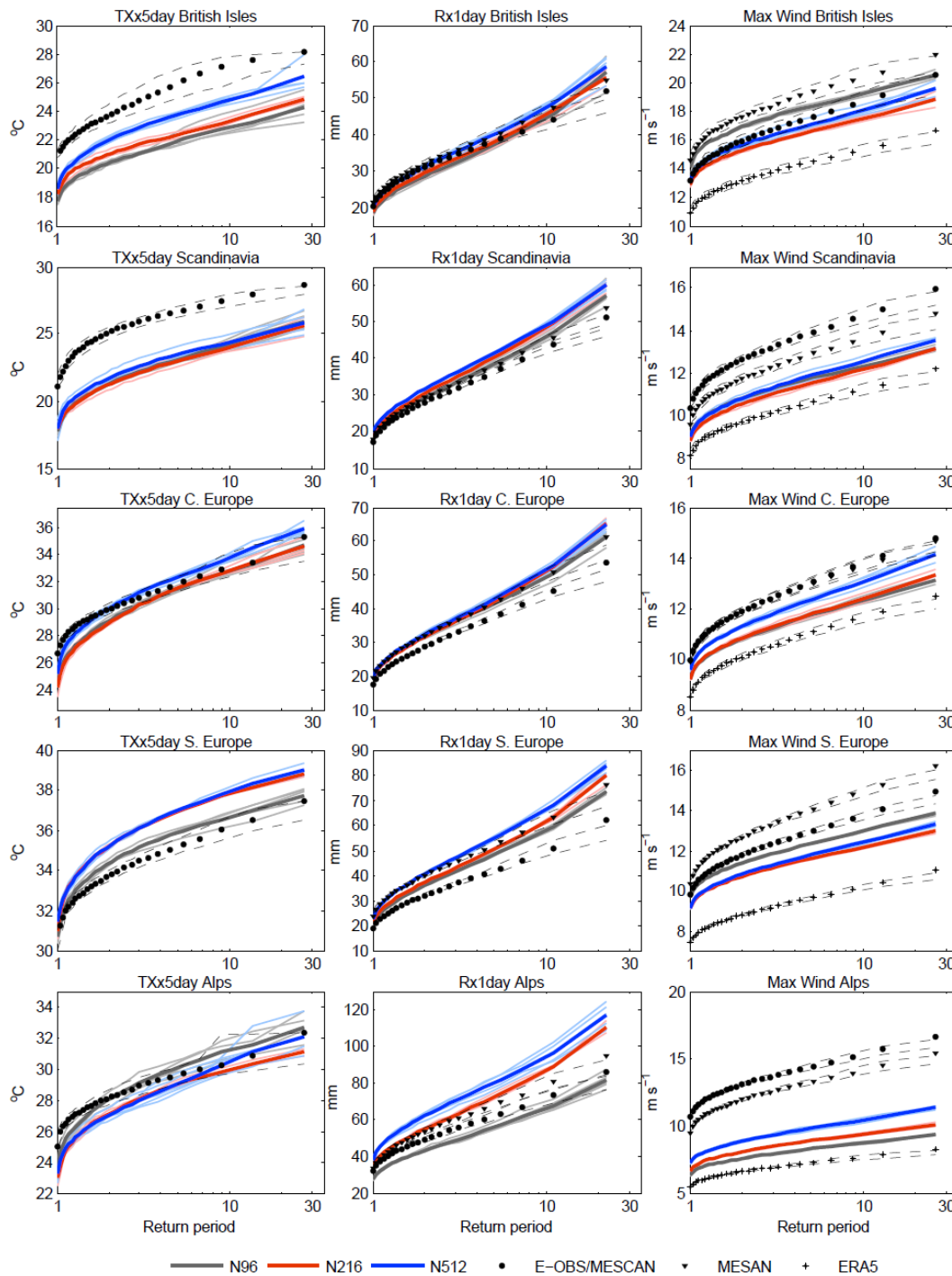


Figure 5: Climatological mean of Txx5day for the ensemble means of three resolutions of HadGEM3-A (UPSCALE) GCM simulations (left) for the period 1985-2011 and their biases with respect to E-OBS (right). (a) E-OBS, (b, c) N96 (130 km), (d, e) N216 (60 km), (f, g) N512 (25 km). Units °C.



1170

Figure 6: Return period plots for (left) TXx5day, middle column Rx1day and (right) annual maximum wind, for the UPSCALE simulations for (top row) the British Isles, (2nd row) Scandinavia, (3rd row) Central Europe, (4th row) Southern Europe, and (last row) the Alps. N96 is shown in grey, N216 in red and N512 in blue. Thin lines are individual ensemble members, thick lines represent

ensemble means. Observational datasets are shown in black, circles for E-OBS and MESHAN, triangles for MESHAN and DYNAD, and asterisks for ERA5. Confidence intervals based on bootstrapping are shown with dashed lines for the observational datasets. The time periods considered are 1985-2011 for TXx5day, 1989-2010 for Rx1day, and 1986-2011 for wind. NB: in contrast to Figure 2 the curves have not been shifted to have the same mean value (see methods), see Figure S10 for the shifted version.

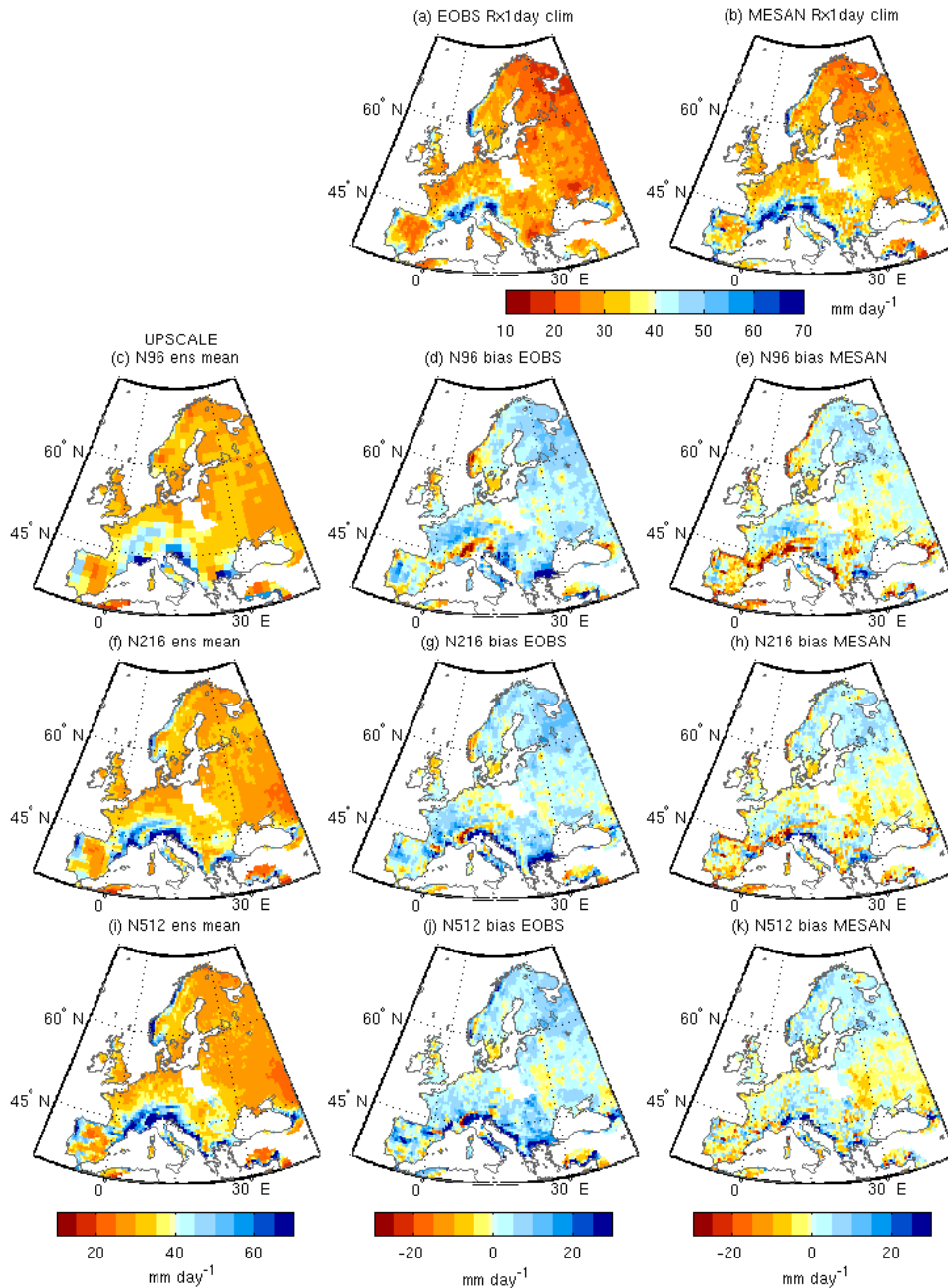


Figure 7: Climatological mean of Rx1day for the ensemble means of three resolutions of UPSCALE (left) simulations for the period 1989-2010 and their biases with respect to E-OBS (middle) and the MESAN reanalysis (right). (a) E-OBS, (b) MESAN (c-e) N96, (f-h) N216, (i-k) N512. Units mm.

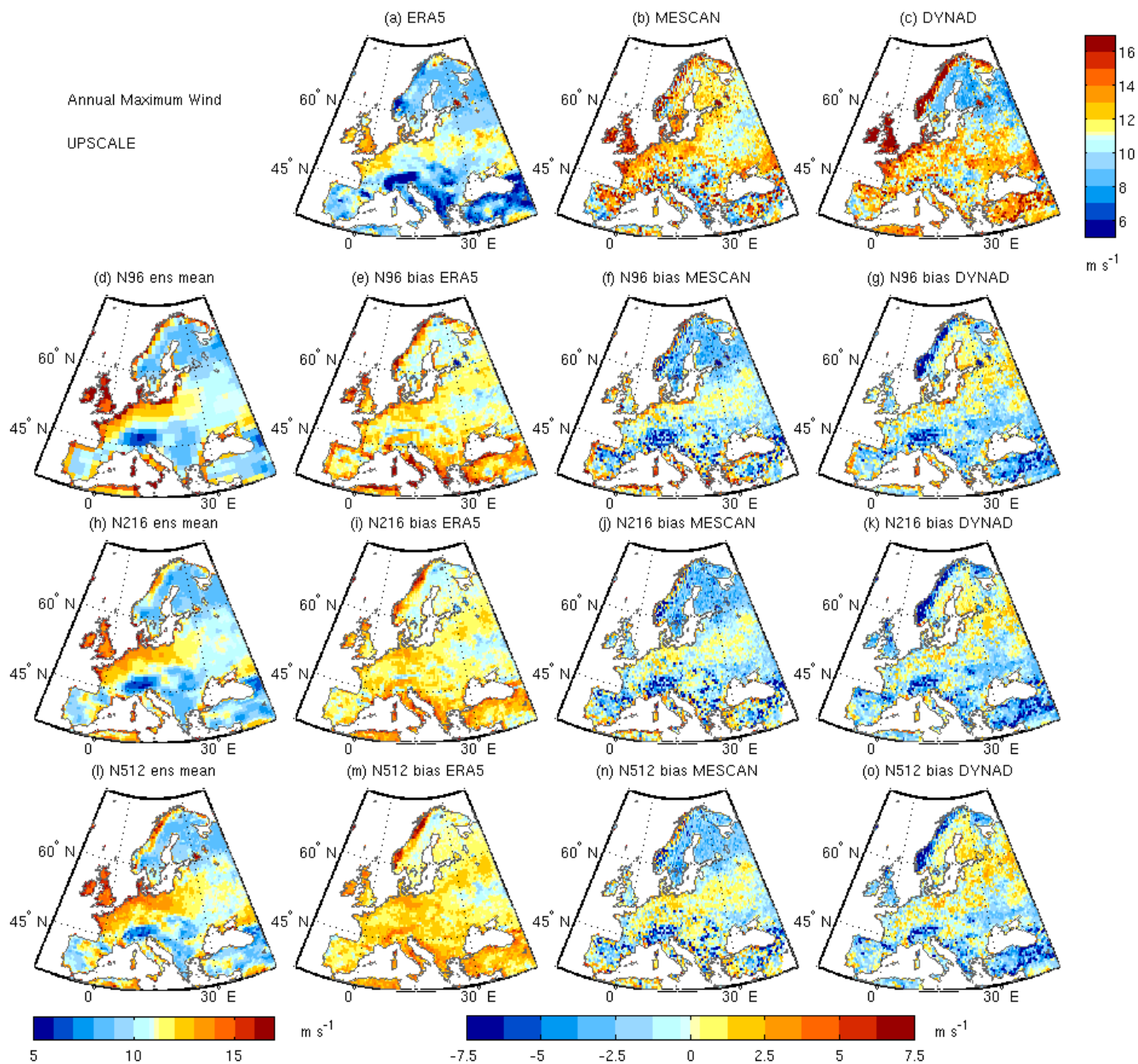
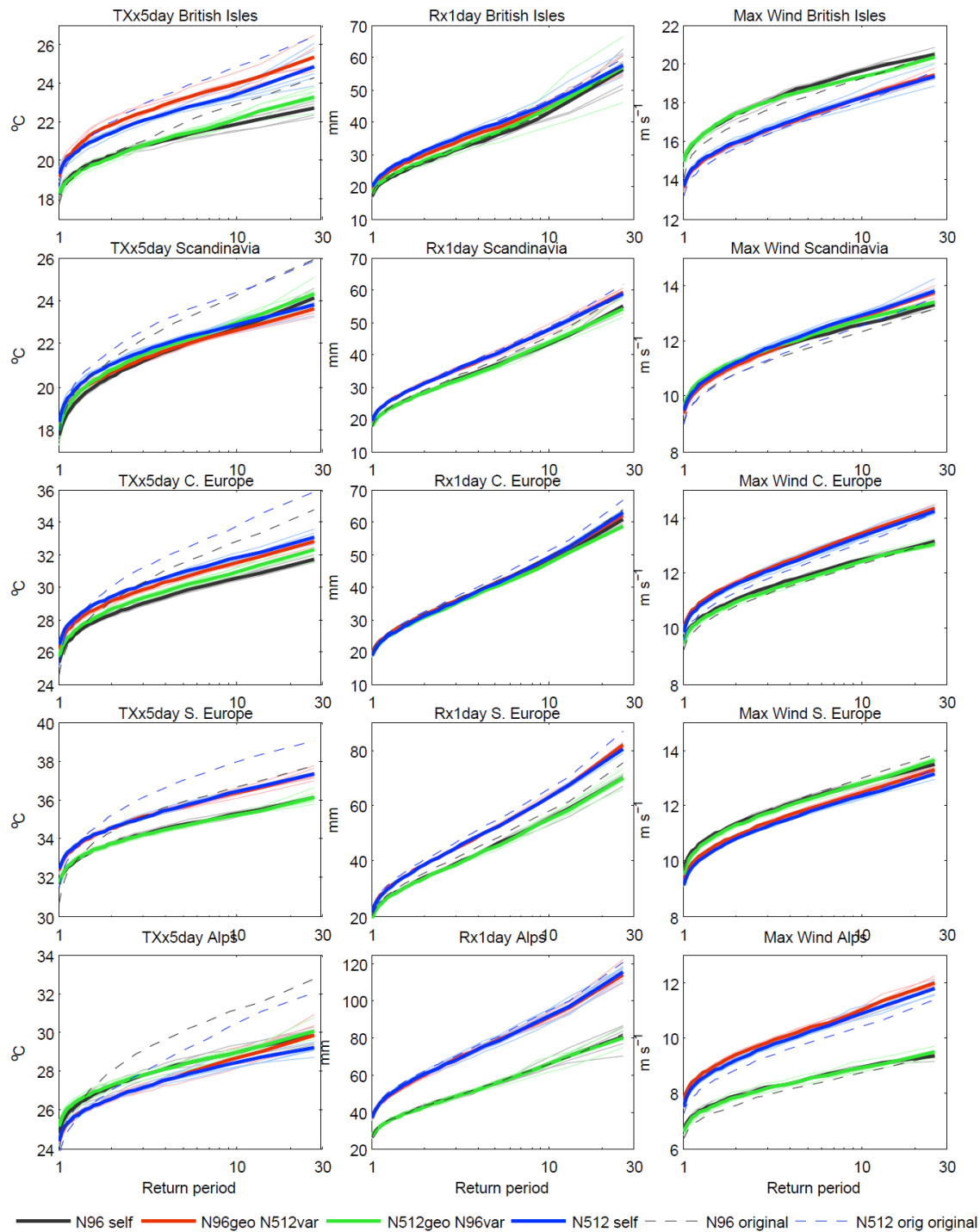


Figure 8: Climatological mean of annual maximum wind for the ensemble means of three resolutions of UPSCALE (left) simulations for the period 1986-2011 and their biases with respect to the observational datasets ERA5 (left column), MESCAN (middle) and MESAN (right). (a) ERA5, (b) MESCAN (c) DYNAD, (d-g) N96, (h-k) N216, (l-o) N512. Units meters per second.



1185

Figure 9: Circulation analogue results. Return period plots for (left) TXx5day, (middle) Rx1day and (right) annual maximum wind for (top) the British Isles, (2nd row) Scandinavia, (3rd row) Central Europe, (4th row) Southern Europe and (5th row) the Alps. Grey represents the N96 self-analogues, blue the N512 self-analogues, red is for N96 circulation with N512 variables (e.g. precipitation)

1190 and green is for N512 circulation with N96 variables. Thin lines represent individual ensemble members, thick lines represent the
mean across individual ensemble members. Blue dashed line represents the original N512 ensemble mean results like those shown
in Figure 6 (although sometimes based on a different time period), and the grey dashed lines represent the equivalent for the N96
simulations. Results for TXx5day are based on the period 1985-2011, Rx1day 1986-2011, and wind 1986-2011.

1195